

1 **Uukuniemi virus as a tick-borne virus model**

2 **Magalie Mazelier¹, Ronan Nicolas Rouxel^{2,#}, Michael Zumstein^{3,&}, Roberta Mancini³,**
3 **Lesley Bell-Sakyi⁴, Pierre-Yves Lozach^{1,2,3}**

4 From ¹CellNetworks – Cluster of Excellence and Department of Infectious Diseases, Virology,
5 University Hospital Heidelberg, Germany; ²INRS-Institut Armand-Frappier, Université du
6 Québec, Laval, Canada; ³ETHZ, Institute of Biochemistry, Zurich, Switzerland; ⁴The Pirbright
7 Institute, Pirbright, United Kingdom

8 Present address: [#]UR 0892, INRA, CRJ, Jouy-en-Josas, France; [&]ETHZ, Institute of
9 Biogeochemistry and Pollutant Dynamics, Zurich, Switzerland

10 Correspondence: P.Y.L.; E-Mail: pierre-yves.lozach@med.uni-heidelberg.de; Phone +49 6221-
11 56-1328; Fax +49 6221-56-5003

12 Running title: Uukuniemi virus in tick cells

13 Keywords: arbovirus, bunyavirus, glycan, glycosylation, host alternation, phlebovirus, tick, tick-
14 borne virus, Uukuniemi virus, tick cell line

15 **Abstract**

16 In the last decade, novel tick-borne pathogenic phleboviruses in the family *Bunyaviridae*, all
17 closely related to Uukuniemi virus (UUKV), have emerged in different continents. To reproduce
18 the tick-mammal switch *in vitro*, we first established a reverse genetics system to rescue UUKV
19 with a genome the closest to that of the authentic virus isolated from the *Ixodes ricinus* tick
20 reservoir. The IRE/CTVM19 and IRE/CTVM20 cell lines, both derived from *I. ricinus*, were
21 susceptible to the virus rescued from plasmid DNAs and supported production of the virus over
22 many weeks, indicating that infection is persistent. The glycoprotein G_C was mainly highly-
23 mannosylated on tick cell-derived viral progeny. The second envelope viral protein, G_N, carried
24 mostly *N*-glycans not recognized by the classical glycosidases PNGase F and Endo H. Treatment
25 with β -mercaptoethanol did not impact the apparent molecular weight of G_N. On viruses
26 originating from mammalian BHK-21 cells, G_N glycosylations were exclusively sensitive to
27 PNGase F and the electrophoresis mobility of the protein was substantially slower after the
28 reduction of disulfide bonds. Furthermore, the amount of viral nucleoprotein per foci forming
29 units differed markedly whether viruses were produced in tick or BHK-21 cells, suggesting a
30 higher infectivity for tick cell-derived viruses. Together, our results indicate that UUKV particles
31 derived from vector tick cells have glycosylation and structural specificities that may influence
32 the initial infection in mammalian hosts. This study also highlights the importance of working
33 with viruses originating from arthropod vector cells when investigating the cell biology of
34 arbovirus transmission and entry into mammalian hosts.

35 **Importance**

36 Tick-borne phleboviruses represent a growing threat to humans globally. Although ticks are
37 important vectors of infectious emerging diseases, previous studies have mainly involved virus
38 stocks produced in mammalian cells. This limitation tends to minimize the importance of host
39 alternation in virus transmission to humans and initial infection at the molecular level. With this
40 study, we have developed an *in vitro* tick cell-based model that allows production of the tick-
41 borne Uukuniemi virus to high titers. Using this system, we found that virions derived from tick
42 cells have specific structural properties and *N*-glycans that may enhance virus infectivity for
43 mammalian cells. By shedding light on molecular aspects of tick-derived viral particles, our data
44 illustrate the importance of considering the host switch in studying early virus-mammalian

- 45 receptor/cell interactions. The information gained here lays the basis for future research, not only
46 on tick-borne phleboviruses, but on all viruses and other pathogens transmitted by ticks.

47 **Introduction**

48 The *Bunyaviridae* is the largest family of RNA viruses. With over 350 members distributed
49 worldwide and classified into five genera (*Tospovirus*, *Nairovirus*, *Orthobunyavirus*,
50 *Phlebovirus*, and *Hantavirus*), these viruses represent a global threat to public health, livestock,
51 and agricultural productivity (1). Hantaviruses apart, bunyaviruses are mainly transmitted by
52 arthropods including sandflies, mosquitoes, and ticks. In the past five years, a number of
53 emerging tick-borne phleboviruses have been reported in different continents. Severe fever with
54 thrombocytopenia syndrome virus (SFTSV) in Asia and Heartland virus (HRTV) in North
55 America are recent examples of new tick-borne phleboviruses causing severe and often fatal
56 disease in humans (2-5). Other phleboviruses genetically related to SFTSV and HRTV have also
57 been recently isolated from ticks in different parts of the world (6). The increasing number of
58 outbreaks and the apparent wide distribution in tick reservoirs demonstrate that these viruses
59 must be taken seriously as emerging agents of disease. Currently, no vaccines or treatments are
60 approved for human use.

61 Tick-borne phleboviruses are enveloped, roughly spherical with a diameter of about 100 nm,
62 and have a tripartite, single-stranded RNA genome that exclusively replicates in the cytosol (7).
63 The large (L) RNA segment codes for the viral RNA-dependent RNA polymerase L, and the
64 medium (M) segment for the glycoproteins G_N and G_C , both in a negative-sense orientation in
65 the viral genomic RNA (vRNA) (7, 8). In addition to the vector, one of the main distinctions
66 between tick-borne phleboviruses and the phleboviruses vectored by dipterans or mosquitoes is
67 the absence of a sequence encoding a non-structural protein NSm in the M segment (7, 8). The
68 small RNA segment (S) codes for the nucleoprotein N and the non-structural protein NSs in an
69 ambisense manner (7, 8). The proteins N and NSs are translated from subgenomic mRNAs
70 transcribed from the vRNA and the antigenomic, replicative-intermediate RNA (cRNA)
71 respectively (7, 8). In the virions, the protein N is associated with the virus RNA genome and,
72 together with the polymerase L, constitutes the ribonucleoproteins (RNPs) (7). In the virus
73 envelope, the glycoproteins G_N and G_C form spike-like projections responsible for virus
74 attachment to host cells and for acid-activated penetration by membrane fusion from late
75 endosomal compartments (7, 9).

76 During natural transmission to vertebrates, tick-borne phleboviruses are introduced into the
77 skin dermis of hosts following bites by infected ticks. Although ticks are both harmful parasites

78 and vectors of several emerging diseases, not only those caused by phleboviruses, little
79 information on the cell biology of ticks is available (10-14). As a consequence, composition and
80 structure of tick cell-derived phleboviral particles remain largely undefined. Our knowledge of
81 the initial infection of vertebrate hosts, cellular receptors and cell entry is mainly based on the
82 use of virus stocks produced in mammalian cells. SFTSV has been shown to subvert the non-
83 muscle myosin heavy chain IIA for early steps of infection (15). Rhabdoviral particles
84 pseudotyped with the glycoproteins of SFTSV (SFTSV-pp) have been found to infect
85 macrophages (16). Human dendritic cells (DCs) are productively infected by many bunyaviruses,
86 including Uukuniemi virus (UUKV), a phlebovirus originally isolated from the tick *Ixodes*
87 *ricinus* in the 1960s (17-21). To enter and infect DCs, SFTSV-pp and UUKV have been shown
88 to exploit DC-SIGN, a C-type (calcium-dependent) lectin that binds high-mannose *N*-glycans on
89 the viral glycoproteins through its C-terminal carbohydrate recognition domain (CRD) (16, 17).
90 Interactions with L-SIGN, a C-type lectin closely related to DC-SIGN but expressed in liver
91 sinusoidal endothelial cells, have also been recently documented for SFTSV-pp and UUKV (16,
92 22). After binding, SFTSV-pp and UUKV depend on endosomal acidification for penetration and
93 infection (16, 23). UUKV is a late-penetrating virus, belonging to a large group of viruses that
94 depend on late endosomal maturation for productive entry (9, 23).

95 We focus here on UUKV, a virus that shares high sequence homology with SFTSV and
96 HRTV (8, 24, 25). However, UUKV is not associated with any disease in humans and is a
97 validated BSL2 surrogate for arthropod-borne bunyaviruses of higher biosafety classification
98 (26). Major advances into various aspects of the phlebovirus life cycle, including virion
99 structure, receptors, cell entry and assembly, have been achieved through the use of UUKV (9,
100 23, 27-32). To determine whether tick cells support phlebovirus productive infection *in vitro*, and
101 whether tick cell-derived phleboviral particles infect human or other mammalian cells, we
102 rescued UUKV from cDNAs with a genome the closest to that of the authentic virus isolated
103 from ticks. Using this system, we examined infection and virus production in tick cells, assessed
104 the progeny virus for interactions with DC-SIGN expressed in mammalian cells, analyzed the
105 glycans and the electrophoresis mobility of the virus glycoproteins G_N and G_C , and tested the
106 infectivity of viral progeny in mammalian cells.

107 **Materials and methods**

108 **Cells and viruses.** All products used for cell culture were obtained from Life Technologies or
109 Sigma Aldrich. Baby Hamster Kidney cells (BHK-21) were grown in Glasgow's minimal
110 essential medium (GMEM) supplemented with 10% tryptose phosphate broth, 5% fetal bovine
111 serum (FBS), 1% glutaMAX, 100 units.mL⁻¹ penicillin, and 100 µg.mL⁻¹ streptomycin (33).
112 Human B (Raji) and epithelial (HeLa) cells that stably express DC-SIGN were cultured
113 according to ATCC recommendations (17, 34). All mammalian cell lines were grown in an
114 atmosphere of 5% CO₂ in air at 37°C. The tick cell lines IRE/CTVM19 and IRE/CTVM20 were
115 cultured in L-15-based medium in sealed, flat-sided tubes (Nunc) in ambient air at 28°C as
116 reported elsewhere (35-37). The prototype UUKV strain 23 (UUKV S23) was originally isolated
117 from the tick *I. ricinus* in the 1960s (i.e. the virus in tick suspension) (21). The UUKV strain
118 used in this study results from five successive plaque purifications of UUKV S23 in chicken
119 embryo fibroblasts (CEFs) and subsequent passages in BHK-21 cells (38, 39). Virus multiplicity
120 of infection is given according to the titer determined in BHK-21 cells.

121 **Antibodies and reagents.** The mouse monoclonal antibodies 8B11A3, 6G9E5 and 3D8B3 are
122 directed against the UUKV nucleoprotein N and the glycoproteins G_N and G_C respectively (40).
123 The rabbit polyclonal antibodies K1224 and K5 are directed against the UUKV glycoproteins G_N
124 and G_C respectively (41). All of these antibodies were a kind gift from Anna Överby and the
125 Ludwig Institute for Cancer Research (Stockholm, Sweden). The rabbit polyclonal antibody U2
126 has been described previously, and recognizes the UUKV proteins N, G_N, and G_C (17). The
127 neutralizing anti-DC-SIGN mouse monoclonal antibody IgG2a (mAb1621) was purchased from
128 R&D Systems. NH₄Cl and EDTA were obtained from Sigma Aldrich and dissolved in deionized
129 water.

130 **Plasmids.** The expression plasmids pUUK-N and pUUK-L were a kind gift from Anna Överby
131 and code for, respectively, the UUKV nucleoprotein N and polymerase L (39). The cDNAs
132 corresponding to the S, M, and L segments of UUKV were synthesized by RT-PCR from vRNA
133 extracts of purified-virus stock using the reverse transcriptase Superscript III (Life
134 Technologies). Their amplification as a single PCR product was carried out using the Herculase
135 II fusion DNA polymerase (Agilent). The PCR products were then cloned between the murine
136 Pol I RNA polymerase promoter and terminator sequences in the pRF108 vector (a generous gift

137 from Ramon Flick, Bioprotection Systems Corporation) (30). The resulting Pol I-driven plasmids
138 (pRF108-S, pRF108-M, and pRF108-L) encoded each of the antigenomic UUKV RNA
139 molecules (i.e. S, M, and L segments). The point mutation G2386A in the M segment was
140 obtained with the QuikChange XL site-directed mutagenesis kit (Agilent) using the plasmid
141 pRF108-M as a template. The complete list of primers and restriction enzymes used for cloning
142 and mutagenesis is shown in **Table 1**.

143 **Rescue of UUKV from plasmid DNAs.** UUKV was rescued by transfecting BHK-21 cells (0.6
144 $\times 10^6$) with the expression plasmids pUUK-L (1 μg) and pUUK-N (0.3 μg) together with 0.5 μg
145 each of pRF108-S, pRF108-M, and pRF108-L. Transfection was performed in the presence of
146 Lipofectamine 2000 (Life Technologies) using a ratio of 3.8 μL to 1 μg of plasmids in 400 μL of
147 OptiMEM (Life Technologies). One hour post-transfection, complete GMEM medium
148 containing 2% FBS was added to the cells. After 5 days, supernatants were collected, clarified,
149 and titrated as described below. Rescued viruses were passaged a minimum of five times in
150 BHK-21 cells.

151 **Virus titration by focus-forming assay.** Following infection of confluent monolayers with 10-
152 fold dilutions of virus in FBS-free medium, cells were grown in the presence of medium
153 containing 5% serum and supplemented with 0.8% carboxymethyl-cellulose to prevent virus
154 spread. Foci were revealed with a diaminobenzidine solution kit (Vector Laboratories) after a
155 two-step immunostaining with the antibody U2 (1:1,000) and an anti-rabbit horseradish
156 peroxidase-conjugated secondary antibodies (Vector Laboratories) (23).

157 **Deglycosylation.** To assess the glycosylation pattern of the UUKV glycoproteins, virus stocks
158 purified through a 25%-sucrose cushion were denatured and exposed to one of the five
159 following treatments: 1,000 units of Endo H (Promega), 5 units of PNGase F, 0.005 units of α -
160 2(3,6,8,9)-neuraminidase, 0.003 units of β -1,4-galactosidase, and 0.05 units of β -N-
161 acetylglucosaminidase (all enzymes from Merck Millipore) according to the manufacturer's
162 recommendations, and then analyzed by SDS-PAGE on a 4-12% or 10% Bis-Tris Nu-PAGE
163 Novex gel (Life Technologies) and immunoblotting.

164 **Protein analysis.** Viral protein extracts from virus stocks purified through a 25% sucrose
165 cushion were analyzed by SDS-PAGE (Nu-PAGE Novex 4-12% Bis-Tris gel, Life
166 Technologies) and transferred to a PVDF membrane (iBlot transfer Stacks, Life Technologies)

167 (17, 23). When indicated, purified viruses were pre-treated with glycosidases or β -
168 mercaptoethanol (40%). For western blot analysis, the PVDF membranes were first incubated
169 with primary mouse monoclonal antibodies 8B11A3 (1:2,000), 3D8B3 (1:100) or 6G9E5
170 (1:100), or rabbit polyclonal antibodies K5 (1:250-1,000), 1224 (1:500-1,000) or U2 (1:2,000),
171 all diluted in TBS containing 0.1% Tween and 5% milk, and then with an anti-mouse or anti-
172 rabbit horseradish peroxidase-conjugated secondary antibody (1:10,000, Santa Cruz),
173 respectively. Bound antibodies were detected by exposure to enhanced chemiluminescence
174 reagents (ECL, GE Healthcare or Life Technologies). For quantitative detection of viral proteins,
175 membranes were first incubated with the rabbit polyclonal antibody U2 (1:1,000) and then with
176 an anti-rabbit infrared fluorescence (IRDye) secondary antibody and analyzed with the Odyssey
177 Imaging Systems and the software Image Studio (Li-Cor Biosciences).

178 **Infection assays.** Mammalian cells were infected with virus at different MOIs in medium
179 without FBS at 37°C for one hour. Virus supernatant was then replaced by complete culture
180 medium and cultures were incubated for up to 64 hours before fixation. Tick cells were exposed
181 to viruses at different MOIs in culture medium containing FBS at 28°C for up to 48 hours. When
182 used for microscopy, tick cells were seeded on poly-L-Lysin (0.01%)-coated coverslips at 28°C
183 on the day before infection. For inhibition assays, cells were pretreated with inhibitors at
184 different concentrations for 30 min and exposed to UUKV in the continuous presence of the
185 inhibitors. The infection was monitored by either wide-field fluorescence microscopy or flow
186 cytometry.

187 **Flow cytometry.** The flow cytometry-based infection assay has been described previously (23).
188 Briefly, after fixation and permeabilization with 0.1% saponin, infected cells were incubated
189 with the mouse monoclonal antibodies 8B11A3 (1:400), 6G9E5 (1:400) or 3D8B3 (1:500) at
190 room temperature for one hour, washed, and subsequently exposed to Alexa Fluor (AF) 647-
191 conjugated secondary anti-mouse antibodies (1:500, Life Technologies) at room temperature for
192 one hour. When the mouse monoclonal antibody 1621 (25 $\mu\text{g.mL}^{-1}$) was used in infection assays
193 to neutralize DC-SIGN, UUKV-infected cells were immuno-stained with the rabbit polyclonal
194 antibody U2 (1:400) and AF647-conjugated secondary anti-rabbit antibody (1:500, Life
195 Technologies). Flow cytometry-based analysis involved the use of a FACS Calibur cytometer
196 (Becton Dickinson) and Flowjo software (Treestar).

197 **Fluorescence microscopy.** Infected cells were fixed and permeabilized with PBS containing
198 0.1% Triton X-100 (Merck Millipore), incubated with the mouse monoclonal antibody 8B11A3
199 (1:1,000) at room temperature for one hour, washed, and then exposed to AF488-conjugated
200 secondary anti-mouse (1:800, Life Technologies) at room temperature for one hour. Nuclei were
201 subsequently stained with Hoechst 33258 ($0.5 \mu\text{g}\cdot\text{mL}^{-1}$, Life Technologies). Infection was
202 quantified by counting cells in three independent fields and cells were imaged with an Olympus
203 IX81 microscope.

204 **Statistical Analysis.** The data shown are representative of at least three independent
205 experiments. Values are given as the mean of triplicates \pm standard deviation (SD).

206 **Sequencing of the full-length M segment isolated from UUKV-infected ticks.** Questing
207 nymphs of the tick *I. ricinus* were collected in the region of Ramsvik and Hindens Rev (Sweden,
208 2013). Pools of 25 nymphs were homogenized and the total RNA was extracted with a magnetic
209 bead-based protocol as described elsewhere (kind gift of Janne Chirico, National Veterinary
210 Institute, Uppsala, Sweden and Sara Moutailler, ANSES, Maisons-Alfort, France) (42). The
211 cDNA corresponding to the M segment of UUKV was synthesized by RT-PCR with the reverse
212 transcriptase Superscript III (Life Technologies) and the specific primer RT-M (**Table 1**) before
213 amplification as a single PCR product using the pfu DNA polymerase (Promega) and the primers
214 UUKV-M-5NC and UUKV-M-3NC (**Table 1**). PCR products were analyzed with a capillary
215 sequencer by ABI (Eurofins Scientific).

216 **GenBank accession numbers.** The GenBank accession numbers for the nucleotide sequence of
217 the M segment of the tick isolates RVS and HRS are KX219593 and KX219594 respectively.

218 **Results**

219 **Recovery of UUKV S23 from RNA polymerase I (Pol I)-driven plasmid DNAs.** The UUKV
220 lab strain that we used in this study as a template for cloning purposes results from the adaptation
221 of the prototype tick isolate strain 23 (UUKV S23) to BHK-21 cells after successive plaque-
222 purifications in CEFs (21, 38, 39). Compared with the S, M, and L nucleotide sequences
223 published for the original UUKV S23 plaque-purified five times in CEFs (GenBank accession
224 numbers NC_005221.1, NC_005220.1, and NC_005214.1 respectively), we identified only a few
225 mutations in our UUKV lab strain (**Figure 1A**). Most were in the M segment. Over the entire
226 virus genome, only one mutation was conserved, a non-silent substitution (A2386G) in the M
227 transcript (43-45) (**Figure 1A**). In all further experiments, for convenience, UUKV will refer to
228 our current mammalian cell-cultured adapted lab strain, rUUKV to the same virus but rescued
229 from cDNAs, UUKV S23 to the original tick isolate plaque-purified five times in CEFs, and
230 rUUKV S23 to the viral particles produced from plasmids encoding genome sequences identical
231 to those published for UUKV S23 in the late 1980s and early 1990s (43-45).

232 Using a reverse genetics system that relies on the cellular Pol I promoter for the synthesis of
233 viral transcripts, the anti-genomic full-length segments S, M, and L from UUKV were cloned
234 into the vector pRF108, which contains the Pol I promoter and terminator. This system has been
235 successfully employed to synthesize chimeric transcripts of the UUKV segment M (30) and to
236 recover infectious particles of the mosquito-borne phlebovirus Rift Valley fever virus (RVFV)
237 from plasmid DNAs (46, 47). The complete system is depicted in **Figure 1B**. From the plasmids
238 coding for the genome of UUKV, it was possible to obtain all the segments encoding UUKV S23
239 with only one site-directed mutagenesis (G2386A in the M segment). This reversion results in
240 the addition of an arginine instead of a glutamine at position 276 in the sequence of the
241 glycoprotein G_C.

242 As there is no evidence for Pol I promoter activity in tick cells, both rUUKV and rUUKV
243 S23 were first rescued from BHK-21 cells, which are highly permissive to most bunyaviruses.
244 The infectious progenies were detected in the cell culture medium by a focus-forming unit (ffu)
245 assay (**Figure 1C**). Both focus formation and growth properties of the recombinant rUUKV and
246 rUUKV S23 in BHK-21 cells were similar to those of UUKV (**Figure 1C**). Co-transfection of
247 the Pol I-driven full-length S, M, and L plasmids together with plasmids coding for the viral

248 polymerase L and nucleoprotein N, whose expression depends on the cytomegalovirus promoter,
249 was essential for the recovery of infectious particles (data not shown).

250 The level of infectious rUUKV and rUUKV S23 in the cell supernatant remained relatively
251 modest five days after transfection, from thousands to hundreds of thousands tffu.mL⁻¹ (**Figure**
252 **1D**). However, the titers significantly increased over subsequent rounds of amplification in
253 BHK-21 cells and reached a plateau of 10⁷ ffu.mL⁻¹ after 2-3 passages, typical for UUKV (17,
254 23) (**Figure 1E**). To assess the identity of the recombinant virus strains recovered from cDNAs,
255 we used the point reversion G2386A in the M sequence as a genetic marker. Total vRNA from
256 rUUKV or rUUKV S23 was extracted after 5 passages in BHK-21 cells, reverse transcribed, and
257 sequenced with primers spanning the reversion site (**Figure 1F**). The sequencing showed that
258 rUUKV S23 was derived from the transfected plasmids and not from contaminating UUKV.

259 We next analyzed rUUKV particles, infection, replication, and progeny production in BHK-
260 21 cells in comparison to UUKV. When the viruses were subjected to SDS-PAGE and western
261 blotting, all three major structural proteins, namely N, G_N, and G_C, were observed in both
262 rUUKV and UUKV virions (**Figures 2A and 2B**). To monitor infection, we used mouse
263 monoclonal antibodies against each of the newly-synthesized virus nucleoprotein N and
264 glycoproteins G_N and G_C before flow cytometry analysis (**Figure 2C**). Using the N protein
265 expression as readout, we found that the kinetics of rUUKV infection were quite similar to those
266 of UUKV (**Figure 2D**). The increase in the proportion of infected cells over time emphasized
267 that viral replication, and not input virus, was quantified in these assays. A complete cycle, from
268 binding to release of infectious progeny, lasted about 6-7 hours in BHK-21 cells (data not
269 shown) and reached a plateau after 48 hours (**Figure 2E**). Similar results were obtained with
270 rUUKV S23 (data not shown).

271 Taken together, our results show that infectious viruses with genomic RNAs identical to
272 those of the original UUKV S23 can be recovered from cDNAs. In turn, our reverse genetics
273 system can be confidently used to investigate the life cycle of tick-borne phleboviruses in vector
274 tick cells as well as the subsequent transmission and initial infection in mammalian hosts.
275 Because it is the model closest to the authentic tick isolate, we then focused on the recombinant
276 strain rUUKV S23.

277 **Tick cells are persistently infected by UUKV.** rUUKV S23 rescued in BHK-21 cells was then
278 used to infect tick cells and regenerate virions with all the features of the original tick-derived

279 virus (e.g. lipids, glycosylation, etc.). Two cell lines derived from embryos of *I. ricinus*, the tick
280 species from which UUKV was first isolated, were used: IRE/CTVM19 and IRE/CTVM20 (35),
281 obtained from the Tick Cell Biobank at The Pirbright Institute, UK. To determine whether
282 IRE/CTVM19 and IRE/CTVM20 cells support infection by tick-borne phleboviruses, they were
283 exposed to rUUKV S23 for 48 hours and immuno-stained with mouse monoclonal antibodies
284 against the nucleoprotein N of UUKV. Flow cytometry allowed quantitative detection of infected
285 cells. Independent of the tick cell line, nearly 50% of cells were infected at a multiplicity of
286 infection (MOI) of 5 and about 20% at a MOI as low as 1.25 (**Figure 3A**). The sensitivity of tick
287 cells to rUUKV S23 infection was confirmed by fluorescence microscopy after immuno-staining
288 of the newly synthesized virus nucleoprotein N (**Figure 3B**). These experiments showed that
289 both tick cell lines support infection of rUUKV S23.

290 We next assessed infected cells for the production of virus progeny. Although cells were
291 infected, titration of cell-free supernatants collected from challenged tick cells indicated that the
292 production of infectious rUUKV S23 particles was almost nonexistent within the first 24 hours
293 of infection (data not shown). After this period, the amount of infectious progeny produced from
294 both tick cell lines increased over time to reach a plateau value within three weeks (**Figure 3C**).
295 Subculturing of infected tick cells 34, 54, and 74 days post-infection, consisting of the removal
296 of half of the cell suspension and replacement with fresh culture medium, did not result in a
297 decrease in viral progeny production (indicated by black arrows in **Figure 3C**). At this time, no
298 cytopathic effects were observed following subculture and the cells grew normally. At 100 days
299 post-infection, high levels of infectious virus were still detectable despite the subculturing of
300 cells. Similar results were obtained when rUUKV was used to infect IRE/CTVM19 and
301 IRE/CTVM20 cells (**Figure 3D**). After several months of amplification in tick cells, the
302 reversion G/A introduced at the position 2386 in the M segment was still present in the genome
303 of rUUKV S23, but not in that of rUUKV (data not shown). Altogether these data indicate that *I.*
304 *ricinus* cells support persistent infection by recombinant UUKV.

305 **Mammalian cells support infection by rUUKV S23 grown in tick cells.** To examine whether
306 rUUKV S23 derived from tick cells remains able to infect mammalian cells, BHK-21 cells were
307 exposed to the viral progeny derived from IRE/CTVM19 cells for 18 hours. Infected cells were
308 analyzed with conformation-dependent mouse monoclonal antibodies in a flow cytometry-based
309 assay. A large proportion of the infected cells were positive for both the virus nucleoprotein N

310 and glycoproteins G_N and G_C (**Figure 4A**), suggesting that infection leads to viral replication.
311 Therefore our phlebovirus-tick cell system appears to be an excellent model for reproducing
312 transmission of tick-borne viruses to mammalian hosts *in vitro*.

313 **DC-SIGN mediates infection by tick cell-derived rUUKV S23.** Due to their presence at the
314 site of initial infection via tick bite, dermal DCs are among the first cells to encounter the
315 incoming viruses (1, 48). We recently established that DC-SIGN, which is highly expressed on
316 the surface of human dermal DCs, binds UUKV directly via interactions with high-mannose *N*-
317 glycans on the virus glycoproteins (17). The capacity of DC-SIGN to bind tick cell-derived viral
318 particles was therefore evaluated using Raji and HeLa cells stably expressing the lectin after
319 transduction with a TRIPAU3 lentiviral vector encoding human DC-SIGN (34). Raji and HeLa
320 cells normally have low or no sensitivity to phlebovirus infection. As expected, parental Raji
321 cells were not detectably infected with IRE/CTVM19 cell-derived rUUKV S23 at a MOI of 5 or
322 less (**Figure 4B**). However, when DC-SIGN was expressed, up to 40% of Raji cells became
323 infected at a MOI of 0.1 (**Figure 4B**). Similarly, fluorescence microscopy analysis of HeLa cells
324 exposed to various MOIs of the virus showed that infection was greatly increased when the lectin
325 was expressed (**Figure 4C**).

326 To confirm that the infection was mediated by DC-SIGN, we utilized the neutralizing mouse
327 monoclonal antibody mAb1621 and EDTA, which inhibits the DC-SIGN binding function by
328 extracting the bound calcium (33). The increase in infectivity due to DC-SIGN expression was
329 significantly reduced in cells treated with inhibitors (**Figure 4D**). Together, these results clearly
330 indicate that infection by tick cell-derived rUUKV S23 is mediated by DC-SIGN and suggest
331 that the viral glycoproteins have, at least in part, high-mannose carbohydrates recognized by the
332 lectin.

333 **G_N and G_C present distinct glycosylation profiles on tick and mammalian cell-derived**
334 **rUUKV S23 particles.** Like other bunyaviruses, UUKV has several *N*-linked oligosaccharides
335 in its envelope glycoproteins G_N and G_C (four sites each). To analyze the glycosylation pattern of
336 G_N and G_C on tick cell-derived viruses, rUUKV S23 was treated with peptide-*N*-glycosidase F
337 (PNGase F) under denaturing conditions before SDS-PAGE and western blotting. When rUUKV
338 S23 was produced in IRE/CTVM19 cells, at least one *N*-glycosylation site on G_N appeared
339 sensitive to PNGase F, while all four sites were sensitive when the virus was derived from BHK-

340 21 cells (**Figure 5A**). In contrast, all four of the *N*-glycans on the glycoprotein G_C were
341 susceptible to the glycosidase regardless of the cells used to produce rUUKV S23 (**Figure 5B**).

342 To further examine the *N*-glycans on rUUKV S23, the virus was subjected to
343 Endoglycosidase H (Endo H). When rUUKV S23 was amplified in BHK-21 cells, the
344 glycoprotein G_N acquired complex glycosylation and was mainly Endo H-resistant (**Figure 5C**),
345 while G_C carried mainly high-mannose *N*-glycans as evidenced by sensitivity to Endo H
346 digestion (**Figure 5D**), i.e. only one site remained resistant. When the virus was produced in the
347 IRE/CTVM19 tick line, both glycoproteins G_N and G_C were sensitive to Endo H, with a
348 digestion pattern identical to that of PNGase F (**Figures 5C and 5D**). These results indicate that
349 all the *N*-glycans on G_N and G_C on tick cell-derived virus particles contain, at least, high-
350 mannose core structures.

351 Of the two viral envelope glycoproteins, G_N shows the most striking differences in
352 glycosylation patterns between tick and BHK-21 cells. To further address these distinctions,
353 rUUKV S23 was exposed to neuraminidase, β -1,4-galactosidase, and β -N-
354 acetylglucosaminidase, which liberate neuraminic acids, β -galactosides, and terminal β -N-
355 acetylglucosamine and N-acetylgalactosamine residues from oligosaccharides, respectively. G_N
356 originating from tick cells, but not from BHK-21 cells, was only sensitive to β -N-
357 acetylglucosaminidase, to a similar extent as PNGase F (**Figures 5E and 5F**). Overall, our data
358 indicate that UUKV particles derived from vector tick cells have glycosylation profiles distinct
359 from those in mammalian cells.

360 **The reduction of di-sulfide bonds impacts the electrophoresis mobility of G_N derived from**
361 **mammalian cells but not from tick cells.** Under reducing and non-reducing conditions, the
362 electrophoretic mobility of G_N on tick cell-derived rUUKV S23 appeared faster than that of the
363 protein on viral particles originating from BHK-21 cells (**Figures 5A and 6A** respectively). In
364 contrast, the electrophoretic mobility of G_C on tick cell-derived virions appeared similar to that
365 of the glycoprotein on viruses produced from BHK-21 cells, under either reducing or non-
366 reducing conditions (**Figures 5B and 6B** respectively).

367 We next assessed whether treatment with β -mercaptoethanol results in a change in the
368 apparent molecular weight of G_N made in tick and mammalian cells. When virions produced in
369 BHK-21 cells were analyzed, the electrophoresis mobility of G_N appeared slower under reducing
370 conditions (**Figure 6C**). In our experimental conditions, no shift was observed when the protein

371 originated from particles derived from tick cells, suggesting that the number of di-sulfide bonds
372 differs between G_N on tick and mammalian cell-derived viruses. Altogether these results suggest
373 that the viral glycoprotein G_N on viruses produced in tick cells has different maturation and
374 folding properties compared to those of the protein on viral particles derived from mammalian
375 cells.

376 **The structural proteins G_N , G_C , and N in infectious viral progeny produced in tick and**
377 **mammalian cells.** We then further examine potential differences in the structure of rUUKV S23
378 particles derived from tick and mammalian cells. For this purpose, viruses were purified through
379 a 25% sucrose cushion, to retain only viral particles with an intact envelope. Identical numbers
380 of infectious particles, based on titration on BHK-21 cells, were analyzed by SDS-PAGE and
381 western blot using the polyclonal antibody U2 against the whole virus, i.e. enabling the detection
382 of G_N , G_C , and N. The amount of nucleoprotein N and glycoproteins G_N and G_C appeared
383 markedly different in virions produced in tick and BHK-21 cells, with substantially less protein
384 N and more glycoproteins G_N and G_C in tick cell-derived viruses (**Figure 7A**).

385 The amount of proteins G_N , G_C , and N incorporated into rUUKV S23 particles was
386 determined by quantitative western blot using the anti-UUKV U2 and an anti-rabbit infrared
387 fluorescence secondary antibody prior analysis with an Odyssey Imaging Systems. The ratio
388 between protein N and ffu was significantly lower in tick cell-derived viruses (**Figure 7B**) while
389 that between the viral glycoproteins and ffu was greater (**Figure 7C**). It was also apparent that
390 the numbers of G_N and G_C molecules per nucleoprotein N (**Figure 7D**) and the number of ffu per
391 N (**Figure 7E**) were higher in virions originating from tick cells. Similar results were obtained
392 with rUUKV (data not shown). From these results, it is most likely that the global structural
393 organization of viral particles exhibit differences between viruses produced in tick and
394 mammalian cells.

395 **Wild type UUKV originating from Swedish ticks in the 2010s.** All RNA viruses are known to
396 have high polymerase error rates. To determine whether the wild type UUKV in vector tick
397 populations has genetically evolved since the 1960s, and thus, whether our tick-borne virus
398 model is still representative of the circulating virus, we analyzed 16 pools of 25 nymphs of the
399 tick *I. ricinus* recently collected in the region of Ramsvik and Hindens Rev (Sweden, 2013) for
400 the presence of the UUKV RNA segment M. The cDNA corresponding to the full-length M
401 segment of UUKV was first synthesized by RT-PCR from vRNA extracted with magnetic beads

402 from nymphal homogenates and then amplified by a single PCR. Out of the 16 homogenates,
403 four were positive, from which it was possible to obtain the full-length nucleotide M sequence
404 for two samples (GenBank accession numbers KX219593 and KX219594). Due to limited
405 amounts of material, a partial sequence only was obtained from one of the two other samples.
406 Nucleotide-sequence analysis showed identity greater than 93% between the UUKV S23 and the
407 virus circulating currently. At the amino-acid level, the sequence identity reached a minimum of
408 98.4%, with 7-11 amino-acid variations located in G_N and 2-4 in G_C (**Table 2**). Together, our
409 data indicates a modest genetic evolution of UUKV glycoproteins in ticks.

410 **Dependence on low pH of rUUKV S23 infectious entry.** We have recently showed in human,
411 rodent, and monkey cells that infectious entry of UUKV is pH-dependent (23). We examined
412 whether the envelope proteins G_N and G_C remain dependent on endosomal acidification to trigger
413 the infectious entry of tick cell-derived viruses into mammalian cells. To this end, DC-SIGN-
414 expressing Raji and HeLa cells were exposed to IRE/CTVM19 cell-derived rUUKV S23 in the
415 presence of agents that neutralize vacuolar pH. The lysomotropic weak base ammonium chloride
416 (NH₄Cl) induced a dose-dependent inhibition of infection in both cell lines (**Figures 8A and**
417 **8B**). Infection of both IRE/CTVM19 and IRE/CTVM20 cells was also sensitive to NH₄Cl
418 (**Figures 8C and 8D**). Similar results were obtained when chloroquine, another lysomotropic
419 agent, was employed (data not shown). These data show that rUUKV S23 infection relies on
420 vacuolar acidification regardless of the host cell origin of the virus and the targeted cell type.

421 **Discussion**

422 Ticks belong to the *Arachnida*, a class distinct from that of insects (*Insecta*) (49, 50). They are
423 arthropods of huge economic significance worldwide, both as harmful ectoparasites and as
424 vectors of many agents of disease, including protozoan and helminth parasites, bacteria, and
425 viruses (10, 50). As obligatory parasites, tick-borne viruses share dependence on biochemical
426 and biophysical features gained in ticks for production in arthropod vectors and then
427 transmission to mammalian hosts and other vertebrates. However, very little is known about the
428 molecular and cell biology of ticks. In the *Bunyaviridae* family, a number of novel pathogenic
429 tick-borne phleboviruses, all closely related to UUKV, have recently emerged in different parts
430 of the world (24, 25). In this context, there is a renewed interest in using UUKV as a model
431 system to examine the initial infection of human hosts by these emerging pathogenic viruses.

432 The orthobunyavirus Bunyamwera virus was the first bunyavirus for which a reverse genetics
433 system was developed to allow the recovery of infectious viral particles from plasmid DNAs
434 (51). Since then, similar or derivative methods have been adapted to some other bunyaviruses,
435 including the tick-borne phlebovirus SFTSV (1, 52-55). In this study, we have added UUKV to
436 the list with a reverse genetics system that relies on the use of the cellular RNA Pol I promoter,
437 enabling modification of the viral genome. The UUKV particles recovered from plasmids were
438 infectious and had replication characteristics similar to those of the authentic virus. An
439 alternative approach to rescuing UUKV from cDNAs that utilizes the T7 promoter was recently
440 described (56). In contrast to this latter method, our Pol I-driven system requires the co-
441 transfection of plasmids coding for the proteins N and L to trigger viral replication and
442 production. This may be explained by the fact that the RNA transcripts under the control of the
443 T7 promoter are exclusively processed in the cytosol, whilst those regulated by the Pol I
444 promoter follow the classical cellular messenger RNA maturation cycle through the nucleus. The
445 main critical advantage of our system concerns the stability of the rescued virus that we showed
446 stable after long-term passage.

447 The reference UUKV strain 23 was isolated from the tick *I. ricinus* in the 1960s and then
448 adapted to tissue culture, being passaged and amplified over many years, first in chicken embryo
449 cells, and subsequently in BHK-21 cells (23, 39, 57). However the nucleotide sequence of the
450 three RNA segments of our UUKV lab strain did not exhibit major evolution compared to that
451 published for the initial virus. As a consequence of this conservation, remarkably high for a RNA

452 virus, it was possible to obtain all the original UUKV RNA transcripts with only one site-
453 directed mutagenesis in the sequence coding for the glycoprotein G_C. In addition, this single
454 mutation does not seem to confer any significant advantages to the virus in terms of infectivity
455 and replication capacity, either in tick or mammalian cells.

456 When UUKV S23 was compared with viruses currently circulating in tick populations, we
457 found a rather modest number of point mutations in the nucleotide sequence of the M segment,
458 which codes for the glycoproteins G_N and G_C. Furthermore, most of these mutations were silent
459 at the amino acid level, with sequence identities reaching 98% and higher. It is not possible to
460 conclude whether the few differences result from (1) the genetic evolution of the virus since the
461 1960s, (2) different sites for the collection of ticks, i.e. Finland for the strain 23 and Sweden for
462 the new isolates, or (3) adaptation of the strain 23 to tissue culture. However, while cloning the
463 circulating virus in our reverse genetics system for future investigations into the new point
464 mutations remains paramount, it is apparent that our tick cells-virus model already allows for
465 addressing many aspects of both the cell biology of ticks and the early steps of initial infection in
466 mammalian hosts, from virus transmission to entry.

467 Several bunyaviruses are vectored by ticks: a few orthobunyaviruses, all the nairoviruses, and
468 all of the phleboviruses related to UUKV (1, 49, 58). While some tick cell lines have been shown
469 to be sensitive to bunyaviruses, including the nairovirus Crimean-Congo hemorrhagic fever
470 virus, we have extended these observations to tick-borne phleboviruses (49). We found that both
471 the IRE/CTVM19 and IRE/CTVM20 cell lines originating from the tick *I. ricinus* are sensitive to
472 UUKV. Both lines supported a complete virus life cycle, from infectious entry to release of new
473 infectious progeny. Although the interaction of additional phleboviruses with tick cell lines must
474 be assessed experimentally, it is likely that many lines can be infected by tick-borne
475 phleboviruses.

476 Arthropod-borne viruses infecting humans and other animals are generally maintained in
477 arthropod vectors and amplified in non-human vertebrates. This is also the case for bunyaviruses
478 (1). In contrast to vertebrate hosts, there is no clear evidence of pathology or lethal outcomes
479 following bunyavirus infection in arthropod hosts. In line with these observations, IRE/CTVM19
480 and IRE/CTVM20 cells infected by UUKV grew normally without any sign of cytopathic effects
481 for many weeks, as reported previously for other arboviruses propagated in tick cell lines (49).
482 Cells exposed to UUKV remained infected for months, demonstrating the asymptomatic

483 persistence of UUKV infection in tick cells. This contrasts with the inability of mammalian cells
484 to survive infection after a couple of days. In UUKV, we have found a suitable surrogate to study
485 important emerging tick-borne pathogens such as SFTSV and HRTV in both tick vectors and
486 mammalian host cells, as well as to reproduce host alternation *in vitro*.

487 Previous studies have mainly involved virus stocks produced in mammalian cells. As a
488 consequence, tick-arbovirus interactions are poorly understood at the cellular level, and the
489 characteristics of viral particles produced from ticks are largely unknown. Using our model
490 system to produce UUKV particles with a genome and biophysical properties very close to those
491 of the virus isolated from ticks, we applied immunoblot-based approaches to analyze the
492 envelope glycoproteins G_N and G_C on tick cell-derived progeny virions. To different extents,
493 both UUKV glycoproteins were sensitive to PNGase F treatment. This highlights the presence of
494 classical *N*-glycan structures on tick cell-derived viral glycoproteins, at least in part.

495 After synthesis in rodent cells, all of the eight *N*-glycosylation sites in the UUKV envelope
496 proteins G_N and G_C have previously been found to carry oligosaccharides, mainly high-mannose
497 glycans (17, 23, 29). In the present study, DC-SIGN enhanced infection of human cells by
498 viruses isolated from tick cells, indicating the existence of high-mannose *N*-glycans on tick cell-
499 derived glycoproteins. The sensitivity of G_N and G_C to Endo H confirmed this presence. It is
500 reasonable to assume that tick cell-derived viruses have the capacity to target cells expressing
501 such lectinic virus receptors in the skin dermis, following introduction into humans and other
502 vertebrates by infected ticks, and before subsequent spread throughout the host.

503 The glycoprotein G_N was much less sensitive to PNGase F and Endo H when the virus was
504 isolated from IRE/CTVM19 cells than from BHK-21 cells. In addition, the β -*N*-
505 acetylglucosaminidase recognized G_N glycosylations only on tick cell-derived virions. Though
506 we cannot completely exclude differential glycosylation processes in tick cells, our data rather
507 support the view that tick cell-derived G_N carries atypical glycans, not recognized by the
508 classical glycosidases PNGase F and Endo H. Very little is known about the nature of
509 oligosaccharides on tick-derived glycoproteins (14, 59). Specific tick glycans may impact the
510 initial infection of human hosts in the skin dermis by broaden the spectrum of potential receptors
511 and target cells or by influencing subsequent entry pathways, especially those mediated by lectin
512 receptors. For instance, DC-SIGN is able to trigger selective signal transduction pathways, which
513 depend on the nature and glycosylation pattern of the captured antigens (60, 61). UUKV can use

514 distinct lectin receptors for entering cells through different mechanisms (22). With regards to
515 this, elucidating the type of glycans synthesized in tick cells and on derivative viruses remains of
516 paramount importance.

517 Both glycoproteins G_N and G_C on virions originating from BHK-21 cells showed molecular
518 features distinct from those on viruses produced in tick cells. G_C differed by one *N*-glycan site,
519 which remained insensitive to Endo H in BHK-21 cells. The glycoprotein G_N had the highest
520 degree of dissimilarity, with striking differences in glycans but also in electrophoresis mobility
521 under reducing and non-reducing conditions. The apparent molecular weight of G_N was lower for
522 viruses produced in IRE/CTVM19 cells than in BHK-21 cells. No deletion in the virus genome
523 segment M, which could explain the translation of a smaller sized protein, was found after
524 several weeks of virus propagation in tick cells (data not shown). Smaller size of glycan units or
525 divergent transcription and maturation processes in tick cells may be responsible for the variation
526 in molecular weight. In addition, that only BHK-21 cell-derived G_N molecules were sensitive to
527 β -mercaptoethanol indicate a difference in the number of di-sulfide bonds between the protein
528 made in tick and mammalian cells. It is likely that the folding of G_N on virions differs depending
529 on whether they are produced in tick or mammalian cells.

530 It is clear from our data that viral particles derived from IRE/CTVM19 and BHK-21 cells
531 exhibit substantial differences in the amount of viral structural proteins, with less nucleoprotein
532 N and more glycoproteins G_N and G_C on virions produced in tick cells. It is tempting to postulate
533 that the level of N protein correlates with the quantity of RNPs and the number of particles, and
534 therefore, that the ratio between ffu and N reflects the ratio between infectious and non-
535 infectious particles. This ratio is known to be low for phleboviruses produced in mammalian
536 cells (23). Though additional experiments are needed to confirm this model, production in tick
537 cells arguably confers an advantage in terms of infectivity to the virus, i.e. with a higher ratio
538 between infectious and non-infectious particles.

539 The ratio between the nucleoprotein N and the glycoproteins G_N and G_C for tick cell-derived
540 viruses significantly differs from that for viral particles produced in mammalian cells. It is
541 reasonable to believe that virions originating from tick cells present an overall structure different
542 from that of the particles derived from mammalian cells. Electron microscopy pictures and
543 tomography-based approaches have shown pleomorphic virions heterogeneous in size for UUKV
544 produced in BHK-21 cells, with spike-like projections of 5-10 nm composed of the two

545 glycoproteins G_N and G_C (27, 32). Structural analyses of UUKV and other tick-borne viruses
546 obtained from arthropod vector cells are still lacking.

547 As with other bunyaviruses, tick-borne phleboviruses rely on vacuolar acidification for
548 infectious entry into mammalian cells (1, 9, 16, 23). The fusion of the virus envelope with the
549 cell membranes is triggered following the acidic activation of the viral glycoproteins. We found
550 that the presence of NH_4Cl resulted in blocking UUKV infection of DC-SIGN-expressing human
551 cells by tick cell-derived viral particles, and of both tick cell lines by viruses produced from
552 BHK-21 cells. In other words, regardless of the host cells that are targeted and those from which
553 the virus originates, UUKV depends on low pH for penetration and infection. Structural data
554 support the view that the phlebovirus glycoprotein G_C is the fusion protein (class II) (62). The
555 possible roles of G_N in the entry and fusion processes of UUKV and other tick-borne
556 phleboviruses, and also in host alternation, remain to be uncovered.

557 The lipid composition of the viral envelope, adaptive mutations in the virus genome, and the
558 nature of oligosaccharides in the virus glycoproteins on tick cell-derived viruses arguably
559 influence the initial infection in humans and other vertebrates, and subsequent spread throughout
560 the host. Tick cell lines and UUKV provide an interesting, functional model to investigate not
561 only tick-borne phleboviruses, but many other intracellular pathogens transmitted by ticks. The
562 results gained here will open avenues in research on tick vectors, the detailed cell biology of
563 which remains a challenge for future work.

564 **Acknowledgments**

565 This work was supported by grants from CellNetworks Research Group funds, the Natural
566 Sciences and Engineering Research Council of Canada #419538-2012, and the Banting Research
567 Foundation to P.Y.L. This work was also supported by the Swiss National Foundation and ETH
568 Zurich. L.B.S. is supported by United Kingdom Biotechnology and Biological Sciences
569 Research Council funding provided to The Pirbright Institute. We thank Ari Helenius for helpful
570 discussions and support.

571 **References**

- 572 1. **Leger P, Lozach PY.** 2015. Bunyaviruses: from transmission by arthropods to virus entry
573 into the mammalian host first-target cells. *Future Virology* **10**:859-881.
- 574 2. **McMullan LK, Folk SM, Kelly AJ, MacNeil A, Goldsmith CS, Metcalfe MG, Batten**
575 **BC, Albarino CG, Zaki SR, Rollin PE, Nicholson WL, Nichol ST.** 2012. A new
576 phlebovirus associated with severe febrile illness in Missouri. *N Engl J Med* **367**:834-841.
- 577 3. **Yu XJ, Liang MF, Zhang SY, Liu Y, Li JD, Sun YL, Zhang L, Zhang QF, Popov VL,**
578 **Li C, Qu J, Li Q, Zhang YP, Hai R, Wu W, Wang Q, Zhan FX, Wang XJ, Kan B,**
579 **Wang SW, Wan KL, Jing HQ, Lu JX, Yin WW, Zhou H, Guan XH, Liu JF, Bi ZQ,**
580 **Liu GH, Ren J, Wang H, Zhao Z, Song JD, He JR, Wan T, Zhang JS, Fu XP, Sun LN,**
581 **Dong XP, Feng ZJ, Yang WZ, Hong T, Zhang Y, Walker DH, Wang Y, Li DX.** 2011.
582 Fever with thrombocytopenia associated with a novel bunyavirus in China. *N Engl J Med*
583 **364**:1523-1532.
- 584 4. **Liu S, Chai C, Wang C, Amer S, Lv H, He H, Sun J, Lin J.** 2014. Systematic review of
585 severe fever with thrombocytopenia syndrome: virology, epidemiology, and clinical
586 characteristics. *Rev Med Virol* **24**:90-102.
- 587 5. **Muehlenbachs A, Fata CR, Lambert AJ, Paddock CD, Velez JO, Blau DM, Staples JE,**
588 **Karlekar MB, Bhatnagar J, Nasci RS, Zaki SR.** 2014. Heartland virus-associated death in
589 Tennessee. *Clin Infect Dis* **59**:845-850.
- 590 6. **Wang J, Selleck P, Yu M, Ha W, Rootes C, Gales R, Wise T, Crameri S, Chen H, Broz**
591 **I, Hyatt A, Woods R, Meehan B, McCullough S, Wang LF.** 2014. Novel phlebovirus
592 with zoonotic potential isolated from ticks, Australia. *Emerg Infect Dis* **20**:1040-1043.
- 593 7. **Blakqori G, Bouloy M, Bridgen A, Elliott RM, Frias-Staheli N, Kormelink R, Medina**
594 **RA, Plyusnin A, Sironen T, Spiropoulou CF, Vaheri A, Vapalahti O.** 2011.
595 *Bunyaviridae: Molecular and Cellular Biology.* Caister Academic Press.
- 596 8. **Elliott RM, Brennan B.** 2014. Emerging phleboviruses. *Curr Opin Virol* **5**:50-57.
- 597 9. **Lozach PY, Huotari J, Helenius A.** 2011. Late-penetrating viruses. *Curr Opin Virol* **1**:35-
598 43.
- 599 10. **Estrada-Pena A, de la Fuente J.** 2014. The ecology of ticks and epidemiology of tick-
600 borne viral diseases. *Antiviral Res* **108**:104-128.

- 601 11. **Nuttall PA.** 2009. Molecular characterization of tick-virus interactions. *Front Biosci*
602 (Landmark Ed) **14**:2466-2483.
- 603 12. **Tonk M, Cabezas-Cruz A, Valdes JJ, Rego RO, Rudenko N, Golovchenko M, Bell-**
604 **Sakyi L, de la Fuente J, Grubhoffer L.** 2014. Identification and partial characterisation of
605 new members of the *Ixodes ricinus* defensin family. *Gene* **540**:146-152.
- 606 13. **Senigl F, Grubhoffer L, Kopecky J.** 2006. Differences in maturation of tick-borne
607 encephalitis virus in mammalian and tick cell line. *Intervirology* **49**:239-248.
- 608 14. **Sterba J, Vancova M, Sterbova J, Bell-Sakyi L, Grubhoffer L.** 2014. The majority of
609 sialylated glycoproteins in adult *Ixodes ricinus* ticks originate in the host, not the tick.
610 *Carbohydr Res* **389**:93-99.
- 611 15. **Sun Y, Qi Y, Liu C, Gao W, Chen P, Fu L, Peng B, Wang H, Jing Z, Zhong G, Li W.**
612 2014. Nonmuscle myosin heavy chain IIA is a critical factor contributing to the efficiency of
613 early infection of severe fever with thrombocytopenia syndrome virus. *J Virol* **88**:237-248.
- 614 16. **Hofmann H, Li X, Zhang X, Liu W, Kuhl A, Kaup F, Soldan SS, Gonzalez-Scarano F,**
615 **Weber F, He Y, Pohlmann S.** 2013. Severe fever with thrombocytopenia virus
616 glycoproteins are targeted by neutralizing antibodies and can use DC-SIGN as a receptor for
617 pH-dependent entry into human and animal cell lines. *J Virol* **87**:4384-4394.
- 618 17. **Lozach PY, Kuhbacher A, Meier R, Mancini R, Bitto D, Bouloy M, Helenius A.** 2011.
619 DC-SIGN as a receptor for phleboviruses. *Cell Host Microbe* **10**:75-88.
- 620 18. **Nfon CK, Marszal P, Zhang S, Weingartl HM.** 2012. Innate immune response to Rift
621 Valley fever virus in goats. *PLoS Negl Trop Dis* **6**:e1623.
- 622 19. **Peyrefitte CN, Perret M, Garcia S, Rodrigues R, Bagnaud A, Lacote S, Crance JM,**
623 **Vernet G, Garin D, Bouloy M, Paranhos-Baccala G.** 2010. Differential activation profiles
624 of Crimean-Congo hemorrhagic fever virus- and Dugbe virus-infected antigen-presenting
625 cells. *J Gen Virol* **91**:189-198.
- 626 20. **Connolly-Andersen AM, Douagi I, Kraus AA, Mirazimi A.** 2009. Crimean-Congo
627 hemorrhagic fever virus infects human monocyte-derived dendritic cells. *Virology* **390**:157-
628 162.
- 629 21. **Oker-Blom N, Salminen A, Brummer-Korvenkontio M, Kaeeriaeinen L, Weckstroem**
630 **P.** 1964. Isolation of some viruses other than typical tick-borne encephalitis viruses from
631 *Ixodes Ricinus* ticks in Finland. *Ann Med Exp Biol Fenn* **42**:109-112.

- 632 22. **Leger P, Tetard M, Youness B, Cordes N, Rouxel RN, Flamand M, Lozach PY.** 2016.
633 Differential use of the C-type lectins L-SIGN and DC-SIGN for phlebovirus endocytosis.
634 Traffic doi:10.1111/tra.12393.
- 635 23. **Lozach PY, Mancini R, Bitto D, Meier R, Oestereich L, Overby AK, Pettersson RF,**
636 **Helenius A.** 2010. Entry of bunyaviruses into mammalian cells. *Cell Host Microbe* **7**:488-
637 499.
- 638 24. **Marklewitz M, Handrick S, Grasse W, Kurth A, Lukashev A, Drosten C, Ellerbrok H,**
639 **Leendertz FH, Pauli G, Junglen S.** 2011. Gouleako virus isolated from West African
640 mosquitoes constitutes a proposed novel genus in the family *Bunyaviridae*. *J Virol* **85**:9227-
641 9234.
- 642 25. **Xu B, Liu L, Huang X, Ma H, Zhang Y, Du Y, Wang P, Tang X, Wang H, Kang K,**
643 **Zhang S, Zhao G, Wu W, Yang Y, Chen H, Mu F, Chen W.** 2011. Metagenomic analysis
644 of fever, thrombocytopenia and leukopenia syndrome (FTLS) in Henan Province, China:
645 discovery of a new bunyavirus. *PLoS Pathog* **7**:e1002369.
- 646 26. **Hubalek Z, Rudolf I.** 2012. Tick-borne viruses in Europe. *Parasitol Res* **111**:9-36.
- 647 27. **Overby AK, Pettersson RF, Grunewald K, Huiskonen JT.** 2008. Insights into bunyavirus
648 architecture from electron cryotomography of Uukuniemi virus. *Proc Natl Acad Sci U S A*
649 **105**:2375-2379.
- 650 28. **Meier R, Franceschini A, Horvath P, Tetard M, Mancini R, von Mering C, Helenius A,**
651 **Lozach PY.** 2014. Genome-wide small interfering RNA screens reveal VAMP3 as a novel
652 host factor required for Uukuniemi virus late penetration. *J Virol* **88**:8565-8578.
- 653 29. **Crispin M, Harvey DJ, Bitto D, Halldorsson S, Bonomelli C, Edgeworth M, Scrivens**
654 **JH, Huiskonen JT, Bowden TA.** 2014. Uukuniemi phlebovirus assembly and secretion
655 leave a functional imprint on the virion glycome. *J Virol* **88**:10244-10251.
- 656 30. **Flick R, Pettersson RF.** 2001. Reverse genetics system for Uukuniemi virus
657 (*Bunyaviridae*): RNA polymerase I-catalyzed expression of chimeric viral RNAs. *J Virol*
658 **75**:1643-1655.
- 659 31. **Overby AK, Pettersson RF, Neve EP.** 2007. The glycoprotein cytoplasmic tail of
660 Uukuniemi virus (*Bunyaviridae*) interacts with ribonucleoproteins and is critical for genome
661 packaging. *J Virol* **81**:3198-3205.

- 662 32. **von Bonsdorff CH, Pettersson R.** 1975. Surface structure of Uukuniemi virus. *J Virol*
663 **16**:1296-1307.
- 664 33. **Lozach PY, Lortat-Jacob H, de Lacroix de Lavalette A, Staropoli I, Fong S, Amara**
665 **A, Houles C, Fieschi F, Schwartz O, Virelizier JL, Arenzana-Seisdedos F, Altmeyer R.**
666 2003. DC-SIGN and L-SIGN are high affinity binding receptors for hepatitis C virus
667 glycoprotein E2. *J Biol Chem* **278**:20358-20366.
- 668 34. **Lozach PY, Burleigh L, Staropoli I, Navarro-Sanchez E, Harriague J, Virelizier JL,**
669 **Rey FA, Despres P, Arenzana-Seisdedos F, Amara A.** 2005. Dendritic cell-specific
670 intercellular adhesion molecule 3-grabbing non-integrin (DC-SIGN)-mediated enhancement
671 of dengue virus infection is independent of DC-SIGN internalization signals. *J Biol Chem*
672 **280**:23698-23708.
- 673 35. **Bell-Sakyi L, Zweygarth E, Blouin EF, Gould EA, Jongejan F.** 2007. Tick cell lines:
674 tools for tick and tick-borne disease research. *Trends Parasitol* **23**:450-457.
- 675 36. **Weisheit S, Villar M, Tykalova H, Popara M, Loecherbach J, Watson M, Ruzek D,**
676 **Grubhoffer L, de la Fuente J, Fazakerley JK, Bell-Sakyi L.** 2015. *Ixodes scapularis* and
677 *Ixodes ricinus* tick cell lines respond to infection with tick-borne encephalitis virus:
678 transcriptomic and proteomic analysis. *Parasit Vectors* **8**:599.
- 679 37. **Dyachenko V, Geiger C, Pantchev N, Majzoub M, Bell-Sakyi L, Krupka I, Straubinger**
680 **RK.** 2013. Isolation of canine *Anaplasma phagocytophilum* strains from clinical blood
681 samples using the *Ixodes ricinus* cell line IRE/CTVM20. *Vet Microbiol* **162**:980-986.
- 682 38. **Pettersson R, Kaariainen L.** 1973. The ribonucleic acids of Uukuniemi virus, a noncubical
683 tick-borne arbovirus. *Virology* **56**:608-619.
- 684 39. **Overby AK, Popov V, Neve EP, Pettersson RF.** 2006. Generation and analysis of
685 infectious virus-like particles of uukuniemi virus (*Bunyaviridae*): a useful system for
686 studying bunyaviral packaging and budding. *J Virol* **80**:10428-10435.
- 687 40. **Persson R, Pettersson RF.** 1991. Formation and intracellular transport of a heterodimeric
688 viral spike protein complex. *J Cell Biol* **112**:257-266.
- 689 41. **Veijola J, Pettersson RF.** 1999. Transient association of calnexin and calreticulin with
690 newly synthesized G1 and G2 glycoproteins of uukuniemi virus (family *Bunyaviridae*). *J*
691 *Virol* **73**:6123-6127.

- 692 42. **Moutailler S, Popovici I, Devillers E, Vayssier-Taussat M, Eloit M.** 2016. Diversity of
693 viruses in *Ixodes ricinus* and characterization of a neurotropic strain of Eyach virus. *New*
694 *microbes and new infections* doi:10.1016/j.nmni.2016.02.012.
- 695 43. **Elliott RM, Dunn E, Simons JF, Pettersson RF.** 1992. Nucleotide sequence and coding
696 strategy of the Uukuniemi virus L RNA segment. *J Gen Virol* **73 (Pt 7)**:1745-1752.
- 697 44. **Ronnholm R, Pettersson RF.** 1987. Complete nucleotide sequence of the M RNA segment
698 of Uukuniemi virus encoding the membrane glycoproteins G1 and G2. *Virology* **160**:191-
699 202.
- 700 45. **Simons JF, Hellman U, Pettersson RF.** 1990. Uukuniemi virus S RNA segment:
701 ambisense coding strategy, packaging of complementary strands into virions, and homology
702 to members of the genus *Phlebovirus*. *J Virol* **64**:247-255.
- 703 46. **Gauliard N, Billecocq A, Flick R, Bouloy M.** 2006. Rift Valley fever virus noncoding
704 regions of L, M and S segments regulate RNA synthesis. *Virology* **351**:170-179.
- 705 47. **Billecocq A, Gauliard N, Le May N, Elliott RM, Flick R, Bouloy M.** 2008. RNA
706 polymerase I-mediated expression of viral RNA for the rescue of infectious virulent and
707 avirulent Rift Valley fever viruses. *Virology* **378**:377-384.
- 708 48. **Heath WR, Carbone FR.** 2013. The skin-resident and migratory immune system in steady
709 state and memory: innate lymphocytes, dendritic cells and T cells. *Nat Immunol* **14**:978-
710 985.
- 711 49. **Bell-Sakyi L, Kohl A, Bente DA, Fazakerley JK.** 2012. Tick cell lines for study of
712 Crimean-Congo hemorrhagic fever virus and other arboviruses. *Vector Borne Zoonotic Dis*
713 **12**:769-781.
- 714 50. **Bell-Sakyi L, Attoui H.** 2013. Endogenous tick viruses and modulation of tick-borne
715 pathogen growth. *Front Cell Infect Microbiol* **3**:25.
- 716 51. **Bridgen A, Elliott RM.** 1996. Rescue of a segmented negative-strand RNA virus entirely
717 from cloned complementary DNAs. *Proc Natl Acad Sci U S A* **93**:15400-15404.
- 718 52. **Brennan B, Li P, Zhang S, Li A, Liang M, Li D, Elliott RM.** 2015. Reverse genetics
719 system for severe fever with thrombocytopenia syndrome virus. *J Virol* **89**:3026-3037.
- 720 53. **Blakqori G, Weber F.** 2005. Efficient cDNA-based rescue of La Crosse bunyaviruses
721 expressing or lacking the nonstructural protein NSs. *J Virol* **79**:10420-10428.

- 722 54. **Elliott RM, Blakqori G, van Knippenberg IC, Koudriakova E, Li P, McLees A, Shi X,**
723 **Szemiel AM.** 2013. Establishment of a reverse genetics system for Schmallenberg virus, a
724 newly emerged orthobunyavirus in Europe. *J Gen Virol* **94**:851-859.
- 725 55. **Ikegami T, Won S, Peters CJ, Makino S.** 2006. Rescue of infectious Rift Valley fever
726 virus entirely from cDNA, analysis of virus lacking the NSs gene, and expression of a
727 foreign gene. *J Virol* **80**:2933-2940.
- 728 56. **Rezelj VV, Overby AK, Elliott RM.** 2015. Generation of mutant Uukuniemi viruses
729 lacking the nonstructural protein NSs by reverse genetics indicates that NSs is a weak
730 interferon antagonist. *J Virol* doi:10.1128/JVI.03511-14.
- 731 57. **Ranki M, Pettersson RF.** 1975. Uukuniemi virus contains an RNA polymerase. *J Virol*
732 **16**:1420-1425.
- 733 58. **Elliott RM.** 2014. Orthobunyaviruses: recent genetic and structural insights. *Nat Rev*
734 *Microbiol* **12**:673-685.
- 735 59. **Man P, Kovar V, Sterba J, Strohalm M, Kavan D, Kopacek P, Grubhoffer L, Havlicek**
736 **V.** 2008. Deciphering Dorin M glycosylation by mass spectrometry. *Eur J Mass Spectrom*
737 (Chichester, Eng) **14**:345-354.
- 738 60. **Gringhuis SI, den Dunnen J, Litjens M, van der Vlist M, Geijtenbeek TB.** 2009.
739 Carbohydrate-specific signaling through the DC-SIGN signalosome tailors immunity to
740 *Mycobacterium tuberculosis*, HIV-1 and *Helicobacter pylori*. *Nat Immunol* **10**:1081-1088.
- 741 61. **Gringhuis SI, den Dunnen J, Litjens M, van Het Hof B, van Kooyk Y, Geijtenbeek TB.**
742 2007. C-type lectin DC-SIGN modulates Toll-like receptor signaling via Raf-1 kinase-
743 dependent acetylation of transcription factor NF-kappaB. *Immunity* **26**:605-616.
- 744 62. **Dessau M, Modis Y.** 2013. Crystal structure of glycoprotein C from Rift Valley fever virus.
745 *Proc Natl Acad Sci U S A* **110**:1696-1701.

746 **Figure legends**

747 **Fig 1. Recovery of UUKV from Pol I-driven plasmid DNAs.** (A) The tri-segmented, negative-
748 sense RNA genome of UUKV. The black arrowhead shows the cleavage site in the polyprotein
749 precursor of the glycoproteins G_N and G_C . The black bars indicate the nucleotides found to be
750 mutated in the UUKV laboratory strain relative to UUKV strain 23. The penetrance of each
751 mutation is indicated underneath. Four to five clones were analyzed for each viral genome
752 segment. (B) Schematic representation of the Pol I-driven UUKV rescue system. (C) Focus-
753 forming assay used for the titration of UUKV strains. Examples are shown for the UUKV lab
754 strain (UUKV) and the viruses rescued from plasmid DNAs after five passages in BHK-21 cells
755 (rUUKV and rUUKV S23). After three days of incubation at 37°C, foci were immuno-stained
756 with the rabbit polyclonal antibody U2 against the viral proteins N, G_N , and G_C . (D) rUUKV and
757 rUUKV S23 production 5 days after transfection of plasmids expressing L, M, and S segments
758 under control of the Pol I promoter together with the UUKV L and N expression plasmids
759 pUUK-L and pUUK-N in BHK-21 cells. (E) Titer of rUUKV and rUUKV S23 after rescue (P0)
760 and up to five passages (P1-P5) in BHK-21 cells. ffu: focus-forming units. (F) Sequence analysis
761 of the rUUKV S23 M segment compared to that of rUUKV carried out from vRNA purified
762 extracts after five passages in BHK-21 cells.

763 **Fig 2. Characterization of UUKV rescued from plasmids.** (A) The UUKV lab strain and
764 rUUKV were analyzed by SDS-PAGE and western blotting under reducing conditions using the
765 rabbit polyclonal antibody U2 against the three structural viral proteins N, G_N , and G_C or (B)
766 under non-reducing conditions with the mouse monoclonal antibodies 8B11A3, 6G9E5, and
767 3D8B3 that recognize each of the structural proteins N, G_N , and G_C , respectively. (C) BHK-21
768 cells were exposed to the UUKV lab strain or rUUKV at a MOI of 0.1 for 24 hours. After
769 fixation and permeabilization, infected cells were immuno-stained for N, G_N , and G_C with the
770 mouse monoclonal antibodies 8B11A3, 6G9E5, and 3D8B3, respectively, and analyzed by flow
771 cytometry. (D) Infection of BHK-21 cells by UUKV and rUUKV was monitored over 64 hours
772 using the flow cytometry-based assay used in C. Infection is given as the percentage of N
773 protein-positive cells. (E) Supernatants collected from cells infected at a MOI of 0.1 and at
774 indicated times were assessed for the production of infectious viral progeny by focus-forming
775 assay.

776 **Fig 3. Infection of tick cells by rUUKV and rUUKV S23 is persistent.** (A) Tick cell lines
777 IRE/CTVM19 and IRE/CTVM20 were exposed to BHK-21 cell-derived rUUKV S23 at the
778 indicated MOIs for 48 hours. Infection was analyzed by flow cytometry after immuno-staining
779 against the nucleoprotein N. (B) IRE/CTVM19 and IRE/CTVM20 cells were exposed to various
780 MOIs of rUUKV S23 derived from BHK-21 cells. The next day, infected cells were immuno-
781 stained for the intracellular UUKV nucleoprotein N using the anti-N primary mouse monoclonal
782 antibody 8B11A3 and an AF488-coupled anti-mouse secondary monoclonal antibody (green).
783 Nuclei were stained with Hoescht (blue) and samples analyzed by wide-field microscopy. (C)
784 and (D) IRE/CTVM19 and IRE/CTVM20 cells were exposed to rUUKV S23 (C) and rUUKV
785 (D). 200 μ L of supernatant of infected cells was harvested daily during the first ten days, and
786 every ten days thereafter. The production of infectious viral particles in the supernatant was
787 determined by focus-forming assays. The cells were subcultured in fresh complete medium (1:1)
788 after sampling of the parent cells on days 34, 54, and 74 (black arrows).

789 **Fig 4. The C type lectin DC-SIGN enhances infection of human cells by tick cell-derived**
790 **rUUKV S23.** (A) BHK-21 cells were infected (at a MOI of 0.1) with rUUKV S23 derived from
791 IRE/CTVM19 cells for 18 hours and immuno-stained for N, G_N, and G_C proteins prior to flow
792 cytometry analysis. (B) Parental and DC-SIGN-expressing Raji cells (Raji and Raji DC-SIGN+)
793 were infected with IRE/CTVM19 cell-derived rUUKV S23 and analyzed by flow cytometry 16
794 hours later after immuno-staining against the viral nucleoprotein. (C) Parental and DC-SIGN-
795 expressing HeLa cells (HeLa and HeLa DC-SIGN+) were exposed to various MOIs of
796 IRE/CTVM19 cell-derived rUUKV S23. The next day, infected cells were immuno-stained for
797 the intracellular virus nucleoprotein N using the anti-N primary mouse monoclonal antibody
798 8B11A3 and an AF488-coupled anti-mouse secondary monoclonal antibody (green). Nuclei
799 were stained with Hoescht (blue) and samples analyzed by wide-field microscopy. (D) Raji DC-
800 SIGN+ cells were exposed to IRE/CTVM19 cell-derived rUUKV S23 (MOI ~1) in the presence
801 of inhibitors blocking DC-SIGN, namely EDTA (5 mM) or the neutralizing mouse monoclonal
802 antibody mAb1621 (25 μ g.mL⁻¹). Intracellular viral antigens were detected by immuno-staining
803 with an anti-UUKV rabbit polyclonal antibody followed by incubation with AF647-conjugated
804 secondary antibodies. Infection was analyzed by flow-cytometry 18 hours later and normalized
805 to infection of DC-SIGN-expressing Raji cells in the absence of inhibitor (% of control).

806 **Fig 5. Glycosylation of the rUUKV S23 envelope glycoproteins G_N and G_C on virions**
807 **produced from tick and mammalian cells. (A) to (F)** IRE/CTVM19 and BHK-21 cell-derived
808 rUUKV S23 purified through a 25%-sucrose cushion was reduced and denatured before
809 digestion with PNGase F (A, B, E, and F), Endo H (C and D), or neuraminidase, β -1,4-
810 galactosidase, and β -N-acetylglucosaminidase (E and F). Proteins were analyzed by SDS-PAGE
811 and western blotting using the rabbit polyclonal antibodies K1224 and K5 against linear epitopes
812 in the viral glycoprotein G_N (A, C, E, and F) and G_C (B and D), respectively.

813 **Fig 6. Electrophoretic mobility of the glycoproteins G_N and G_C on rUUKV S23 produced in**
814 **tick and mammalian cells. (A) and (B)** BHK-21 and IRE/CTVM19 cell-derived rUUKV S23
815 purified through a 25%-sucrose cushion were analyzed by non-reducing SDS-PAGE and western
816 blotting, using the mouse monoclonal antibodies 6G9E5 and 3D8B3 against conformational
817 epitopes in G_N (A) and G_C (B) respectively. (C) rUUKV S23 viruses produced in BHK-21 and
818 IRE/CTVM19 cells were purified through a 25%-sucrose cushion and analyzed by non-reducing
819 (-) or reducing (+) SDS-PAGE and western blot with the rabbit polyclonal anti- G_N antibody
820 K1224.

821 **Fig 7. The structural rUUKV S23 proteins G_N , G_C , and N in infectious particles derived**
822 **from tick and mammalian cells. (A)** The amount of viral glycoproteins and N protein for 10^5
823 and $5 \cdot 10^5$ foci forming units (ffu) of purified rUUKV S23, produced in either tick cells or BHK-
824 21 cells, were analyzed by SDS-PAGE and western blot using the rabbit polyclonal anti-UUKV
825 antibody U2, which recognized G_N , G_C , and N. (B) to (E) The amount of viral glycoproteins and
826 protein N for identical amounts of purified infectious rUUKV S23 was determined by
827 quantitative western blot (Odyssey Imaging Systems) with the anti-UUKV U2 and an anti-rabbit
828 infrared fluorescence secondary antibody. The ratios of N protein (B) or viral glycoproteins (C)
829 per ffu and the ratios of viral glycoproteins (D) or ffu (E) per relative unit of N protein are
830 shown.

831 **Fig 8. Low pH dependence of rUUKV S23 for infection. (A) and (B)** Raji (A) and HeLa (B)
832 cells that stably express DC-SIGN were pre-treated with NH_4Cl , a weak base that neutralizes the
833 endosomal pH, and then exposed to IRE/CTVM19 cell-derived rUUKV S23 (MOI ~ 5) in the
834 continuous presence of the inhibitor. Infected cells were harvested 16 hours later and immuno-
835 stained for the UUKV nucleoprotein N. Infection was analyzed by (A) flow cytometry or (B)

836 wide-field microscopy counting at least 200 cells in more than three independent fields. Data
837 were normalized to DC-SIGN-expressing cells infected in the absence of inhibitor (% of
838 control). **(C) and (D)** IRE/CTVM19 (C) and IRE/CTVM20 (D) cells were infected with BHK-21
839 cell-derived rUUKV S23 at a MOI of 5 for 36 hours in the continuous presence of NH₄Cl.
840 Infection was analyzed by flow cytometry and normalized against data obtained in the absence of
841 inhibitor (% of control).

842 **Table 1. Names and sequences of the primers used for cloning and mutagenesis.** Lower case
843 nucleotide letters indicate the virus RNA sequence that is targeted while those in capital letters
844 show the sequences introduced for cloning. Underlined nucleotide sequences indicate a BsmBI
845 restriction site. Bold nucleotides are the point mutation introduced in the M segment sequence of
846 the UUKV lab strain. Forw: forward, Rev: reverse, and RT: reverse transcription.

847 **Table 2. Full-length sequence of the viral glycoproteins G_N and G_C obtained from UUKV-**
848 **infected field *Ixodes ricinus* nymphal ticks.** Total RNAs were extracted from 16 pools of 25
849 nymphs collected in the region of Ramsvik and Hindens Rev Sweden in 2013. The cDNA
850 corresponding to the M segment of UUKV was synthesized by RT-PCR and amplified by a
851 single PCR. Out of the 16 nymphal pools, four were positive for the virus, and from these four
852 samples, one partial and two full-length nucleotide sequences could be obtained and. The list is
853 shown of the amino acids found to be mutated in the full-length amino acid sequences of isolates
854 RVS and HRS (GenBank accession numbers KX219593 and KX219594 respectively) relative to
855 the polypeptide precursor of the two glycoproteins G_N and G_C of UUKV S23 (GenBank
856 accession number NC_005220.1). The point mutations in light gray indicate positive
857 substitutions.

Table 1

Primer	Sense	Sequence (5' -> 3')	Purpose
RT-S	Forw.	acacaaagacctccaacttagctatcg	RT S segment
RT-M	Forw.	acacaaagacggctaacatggtaagg	RT M segment
RT-L	Forw.	acacaaagacgccaagatgcttttagcg	RT L segment
UUKV-S-5NC	Forw.	AATCGTCTCTAGGTacacaaagacctccaacttagctatcg	Cloning S segment into pRF108 (pRF108-S)
UUKV-S-3NC	Rev.	AATCGTCTCTGGGacacaaagacctcc	
UUKV-M-5NC	Forw.	AATCGTCTCTAGGTacacaaagacggctaacatggtaagg	Cloning M segment into pRF108 (pRF108-M)
UUKV-M-3NC	Rev.	AATCGTCTCGGGGacacaaagacacggctacatgg	
UUKV-L-5NC	Forw.	AATCGTCTCTAGGTacacaaagacgccaagatgcttttagcg	Cloning L segment into pRF108 (pRF108-L)
UUKV-L-3NC	Rev.	AATCGTCTCGGGGacacaaagtccgccaagatggaagtaaagg	
Mut-M-S	Forw.	caaggattcagtggttgctc a atcatcaatcatagatccca	Mutagenesis M segment (G2386A)
Mut-M-AS	Rev.	tgggatctatgattgatgat t gacaatccactgaatccttg	

Table 2

Region (start .. end)	Isolate (name)	Identity (%)	Positives (%)	Substitutions relative to the UUKV S23 polypeptide precursor of G _N and G _C (1,008 amino acids)						
G _N (18 .. 496)	RVS	98.5	99.6	L8I	L29I		S124T	T167S	L207V	A219T
	HRS	97.6	98.7		L29I	T44A	S124T	T167S	L207V	A219T
				T237A						
				S282T	T287A	N476K	N477Q	A479C		
Intra region (497 .. 513)	RVS	100.0	100.0							
	HRS	97.1	97.1	A508T						
G _C (514 .. 1008)	RVS	99.6	100.0		S695T	Q790R				
	HRS	99.2	99.8	K577R		Q790R	T841S	L1003F		

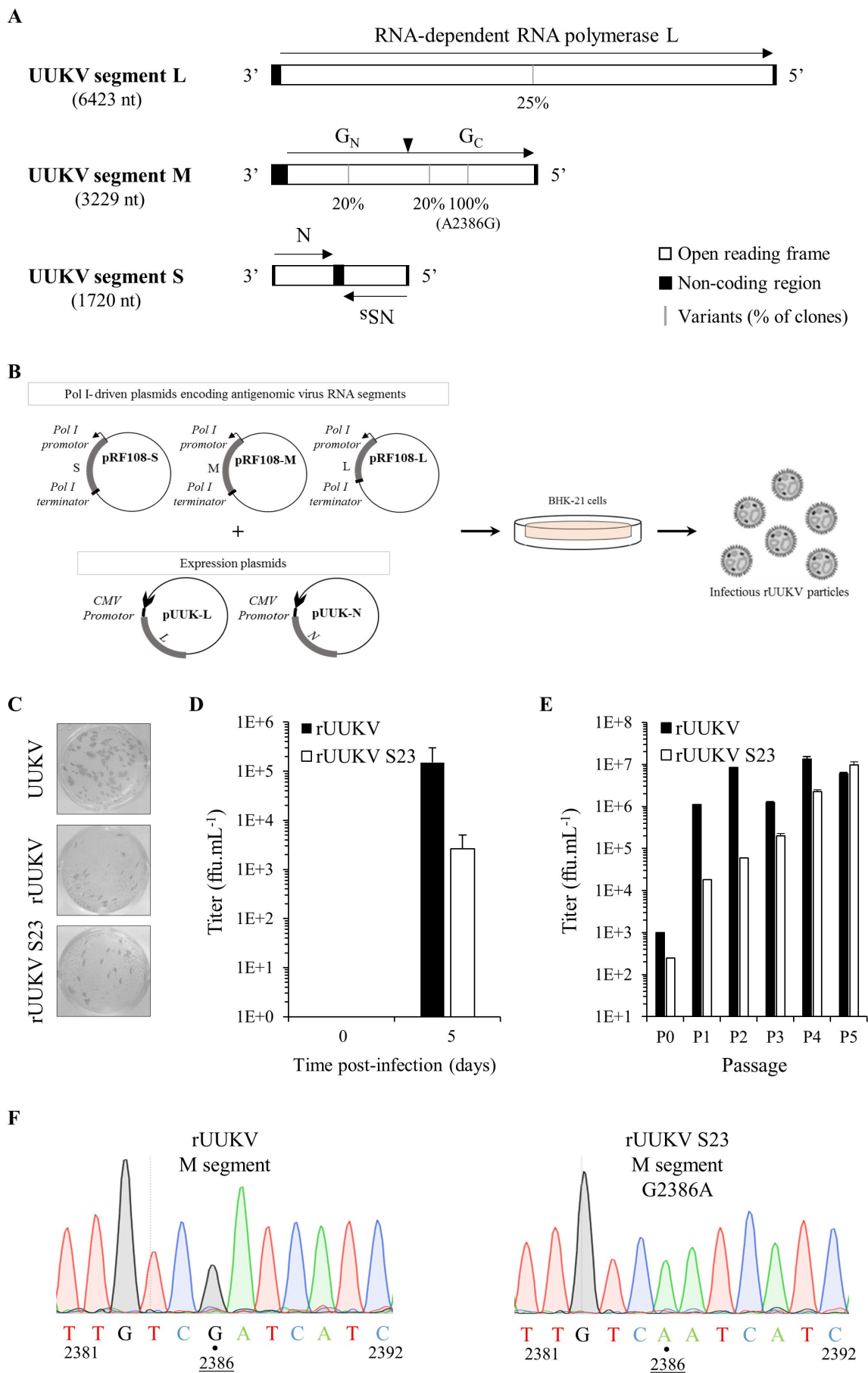


Fig. 1

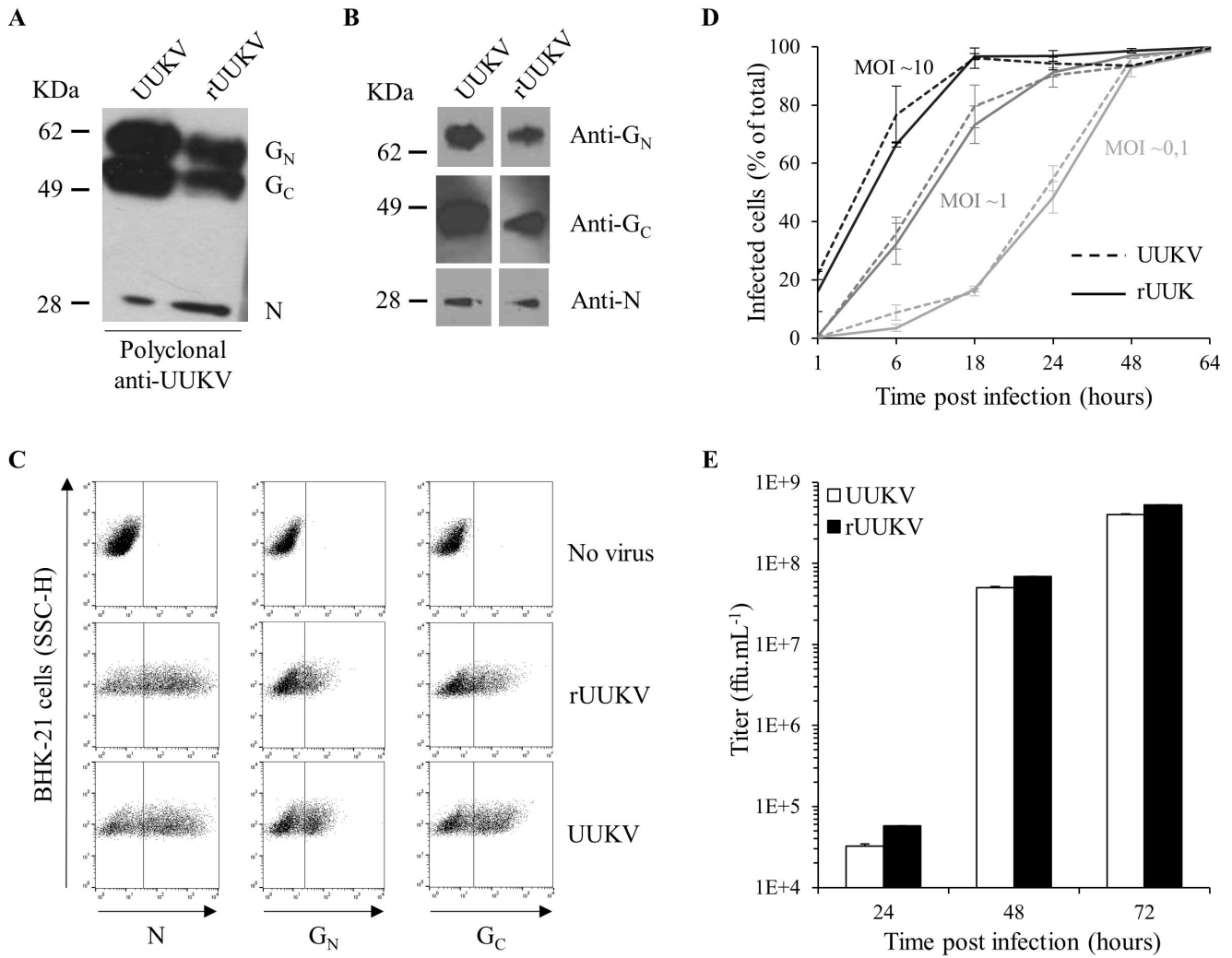


Fig. 2

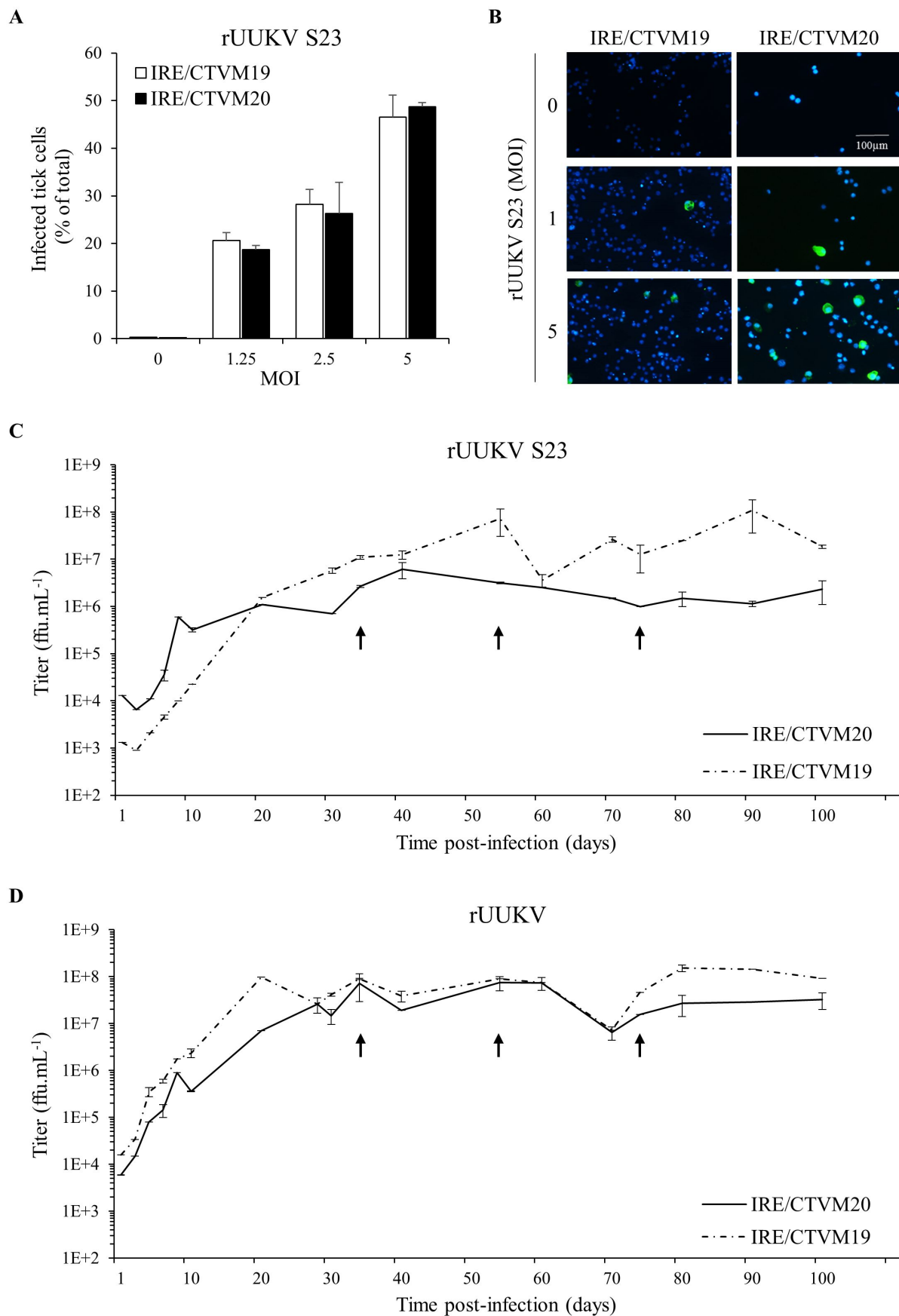


Fig. 3

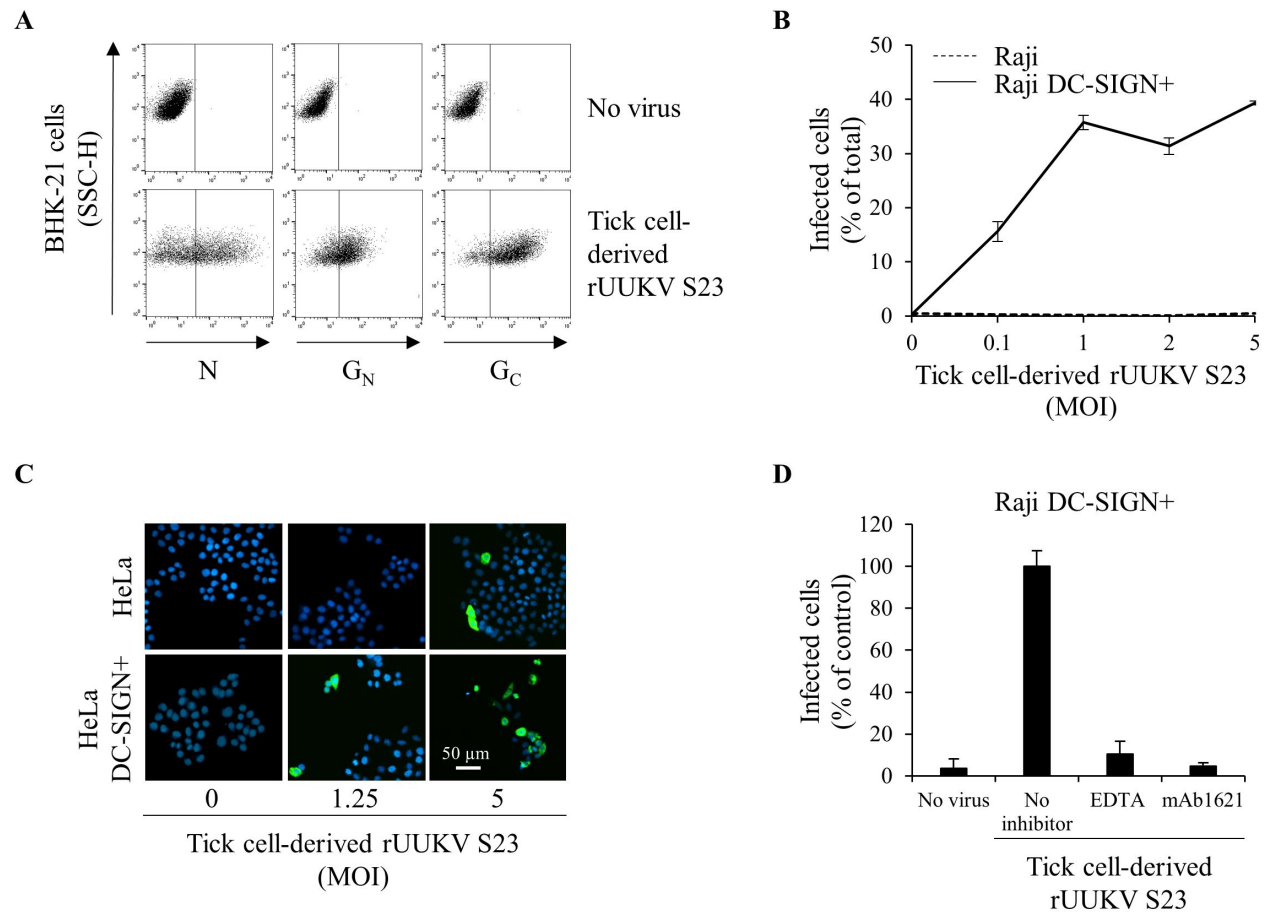


Fig. 4

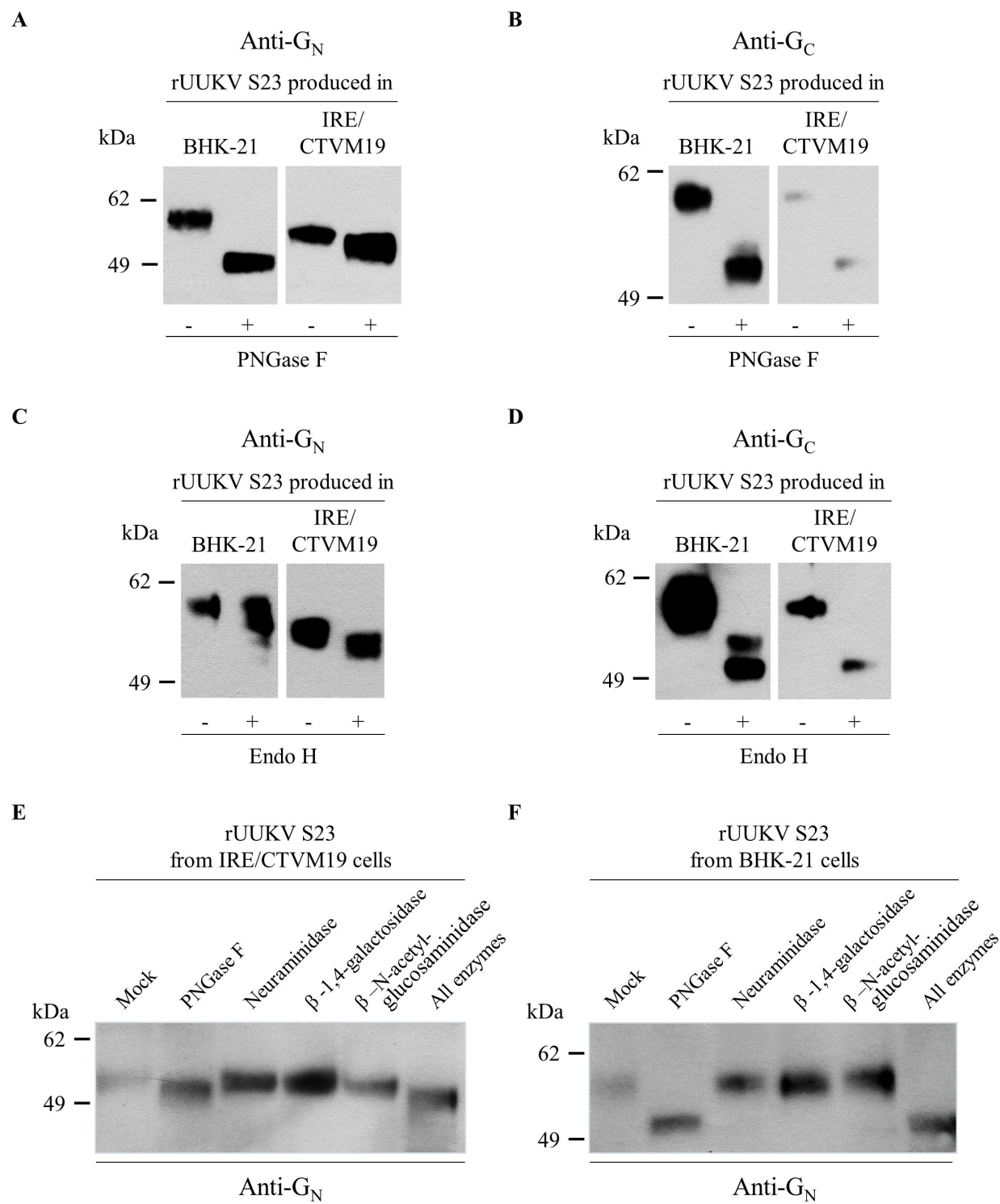


Fig. 5

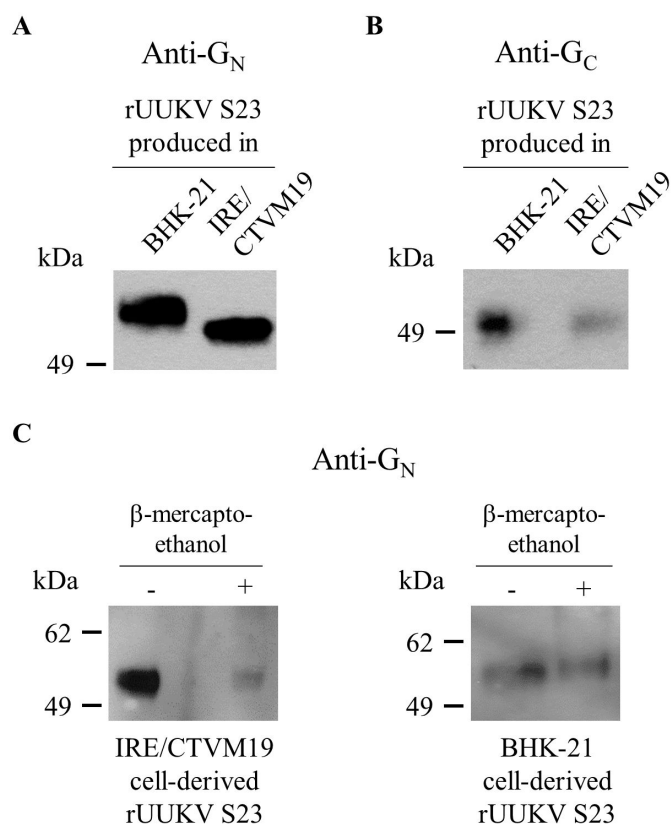


Fig. 6

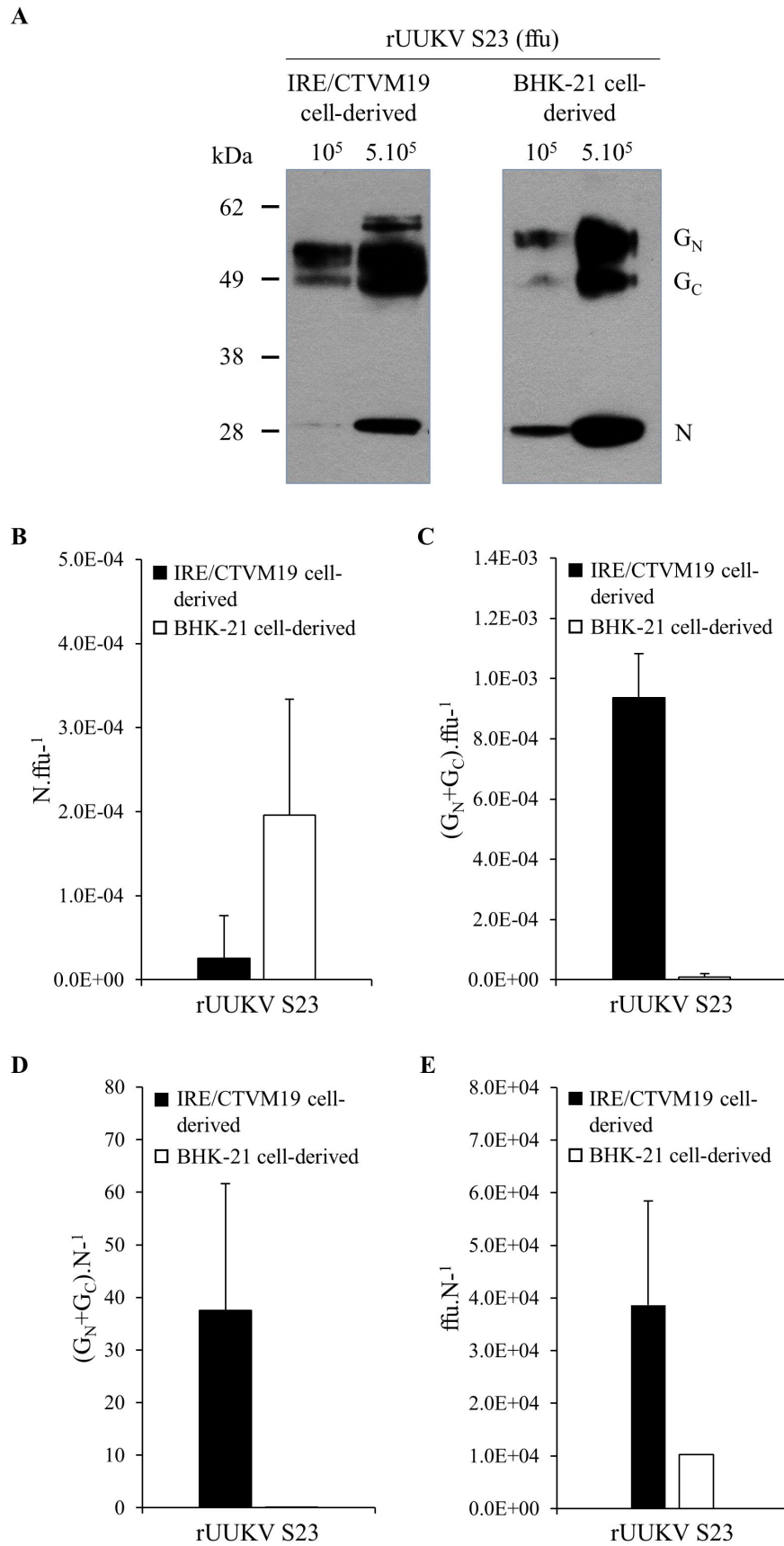


Fig. 7

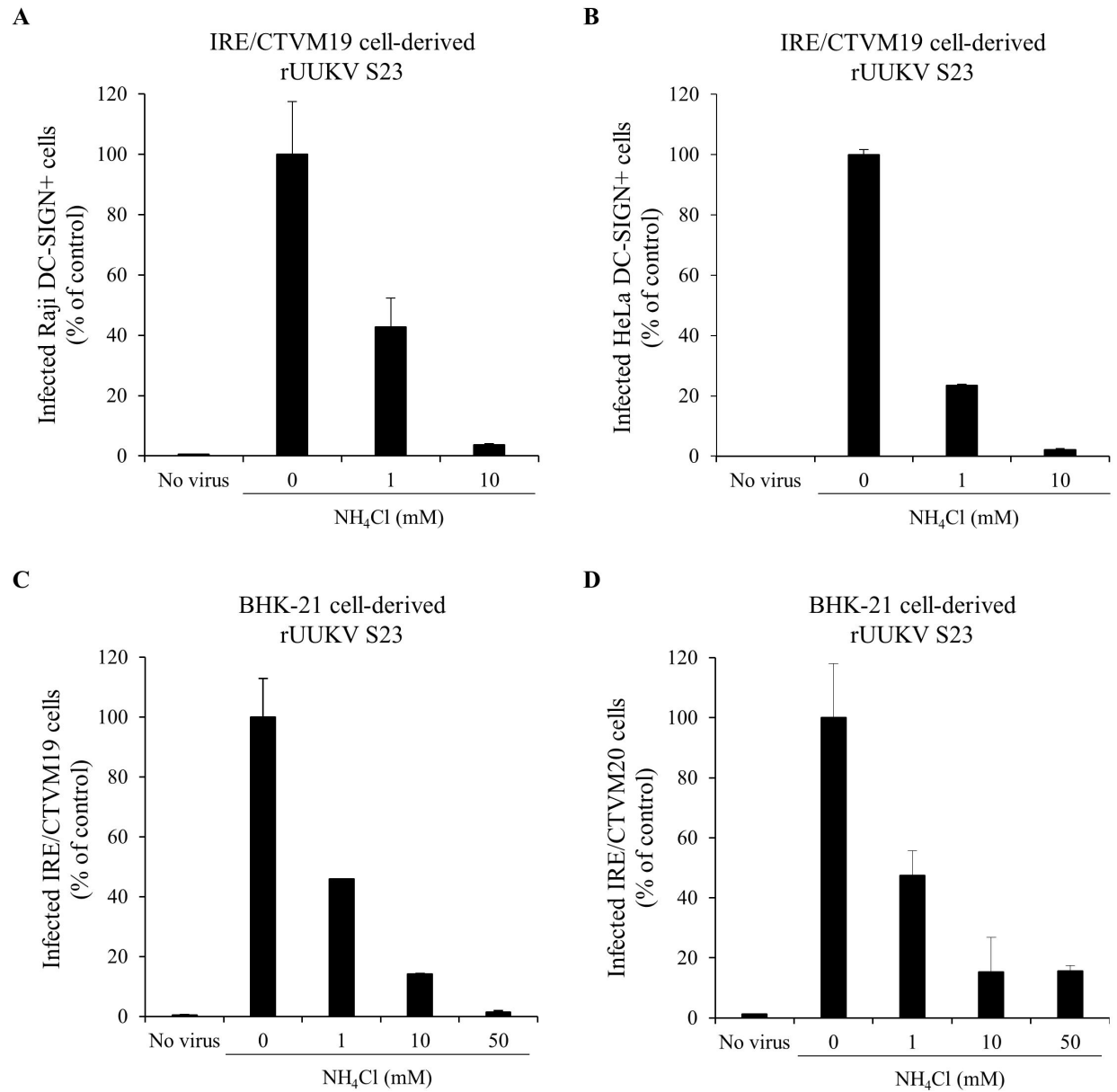


Fig. 8